



Published in final edited form as:

Nat Immunol. 2021 October ; 22(10): 1316–1326. doi:10.1038/s41590-021-01011-2.

Environmental Allergens Trigger Type 2 Inflammation Through Ripoptosome Activation

Michael Brusilovsky¹, Mark Rochman¹, Yrina Rochman¹, Julie M. Caldwell¹, Lydia E. Mack¹, Jennifer M. Felton¹, Jeff E. Habel¹, Aleksey Porollo^{2,3,5}, Chandrashekhar Pasare^{4,5}, Marc E. Rothenberg^{1,5,§}

¹Division of Allergy and Immunology, Cincinnati Children's Hospital Medical Center, Cincinnati, Ohio

²Center for Autoimmune Genomics and Etiology, Cincinnati Children's Hospital Medical Center, Cincinnati, Ohio

³Division of Biomedical Informatics, Cincinnati Children's Hospital Medical Center, Cincinnati, Ohio

⁴Division of Immunobiology, Center for Inflammation and Tolerance, Cincinnati Children's Hospital Medical Center, Cincinnati, Ohio

⁵Department of Pediatrics, University of Cincinnati College of Medicine, Cincinnati, Ohio

Abstract

Environmental allergens including fungi, insects and mites trigger type 2 immunity; however, the innate sensing mechanisms and initial signaling events remain unclear. Herein, we demonstrate that allergens trigger RIPK1-caspase 8 ripoptosome activation in epithelial cells. The active caspase 8 subsequently engages caspases 3 and 7, which directly mediate intracellular maturation and release of IL-33, a pro-atopy, innate immunity, alarmin cytokine. Mature IL-33 maintained functional interaction with the cognate ST2 receptor and elicited potent pro-atopy inflammatory activity in vitro and in vivo. Inhibiting caspase 8 pharmacologically and

Users may view, print, copy, and download text and data-mine the content in such documents, for the purposes of academic research, subject always to the full Conditions of use:http://www.nature.com/authors/editorial_policies/license.html#terms

§Corresponding author: marc.rothenberg@cchmc.org.

Author Contributions

M.B. and M.E.R. designed the study. M.B., M.E.R and C.P. designed experiments. M.B., M.R., Y.R., J.M.C., L.E.M. J.M.F. and J.E.H. performed experiments and data analysis. A.P. performed modeling and protein structure analysis. M.B., M.E.R and C.P. interpreted results and wrote the manuscript. All authors read and commented on manuscript.

Competing Interests Statement

M.E.R. is a consultant for Pulm One, Spoon Guru, ClostraBio, Serpin Pharm, Allakos, Celgene, Astra Zeneca, Adare/Elodi Pharma, Glaxo Smith Kline, Regeneron/Sanofi, Revolo Biotherapeutics, and Guidepoint, and has an equity interest in the first five listed, and royalties from reslizumab (Teva Pharmaceuticals), PEESSv2 (Mapi Research Trust) and UpToDate. M.E.R. is an inventor of patents owned by Cincinnati Children's Hospital. The remaining authors declare no competing interests.

Source Data Set. Supplemental immunoblots for all figures

Full uncropped scans of the immunoblot images for all immunoblots in the Figures 1–6 and Extended Figures 1–8 are shown. Blot images are pasted in and labelled with the relevant panel and protein name identifying information for the antibody used (See Methods; Supplemental Information file). Right margin (throughout): protein names (cl, cleaved; fl, full length; m, mature; p, precursor; tot, total; ph, phosphorylated); # are non-specific bands. The red boxes mark the cropped images shown in the individual figure panels as indicated. Green arrowheads correspond to the membranes cut and separated to incubate with different antibodies and then combined, simultaneously exposed, and scanned together.

deleting murine *Il33* and *Casp8* each attenuated allergic inflammation in vivo. Clinical data substantiated ripoptosome activation and IL-33 maturation as likely contributors to human allergic inflammation. Our findings reveal an epithelial barrier, allergen-sensing mechanism that converges on the ripoptosome as an intracellular molecular signaling platform triggering type 2 innate immune responses. These findings have significant implications for understanding and treating human allergic diseases.

Introduction

Allergic diseases are mediated by the complex interplay between the innate and adaptive immunity.^{1, 2} Although myeloid cells prime adaptive immunity in generating IgE³ and type 2 T helper cell (Th2) responses,⁴ how allergens are initially recognized by the innate immune system, triggering downstream responses leading to production of type 2 effectors, prior to the initiation of adaptive immunity remains unknown.

Myeloid lineage cells express pattern recognition receptors (PRRs)⁴ that recognize both pathogen- and damage-associated molecular patterns (PAMPs and DAMPs, respectively), which are broadly shared across kingdoms⁵ and initiate polarized T helper (Th) cell responses.^{4, 6} Dendritic cell-expressed PRRs (e.g., TLR4) and diverse C-type lectin receptors have been implicated in recognizing allergen-associated PAMPs.^{2, 7} Yet, myeloid cells sensing allergens is likely secondary to the primary breach of the mucosal barrier; myeloid cells respond to effectors produced by mucosal epithelial cells, thus inducing an indirect response via PRR-dependent mechanisms.⁸

The epithelium constitutes a key component of the innate immune system, providing a physical and immune-modulatory barrier that is a first line of defense against environmental agents.^{9, 10} It generates a range of mediators promoting inflammation, barrier dysfunction and mucosal remodeling.¹¹ Epithelium-derived IL-33, an IL-1 superfamily alarmin cytokine,^{12, 13} has a pleotropic role in promoting the development of allergic responses. It functions via IL-1RL1 (ST2)-mediated activation of innate lymphoid type 2 cells (ILC2), Th2 cells, neutrophils, mast cells and eosinophils.^{12, 13, 14} Furthermore, *IL33* and *ST2* genetic variants associate with allergy susceptibility.¹⁵ Though IL-33 is stored in the nucleus, it has been proposed that precursor IL-33 may be released upon cellular injury¹⁶ and subsequently undergo extracellular maturation and activation by neutrophil, mast cell or allergen-derived, non-specific serine proteases.^{12, 13} However, the paradigm of protease-activated IL-33 does not explain how IL-33 is initially released and does not account for the influx of immune cells before IL-33 release. How epithelial cells respond to allergens, particularly in the context of type 2 alarmin (e.g., IL-33) production, is not well understood. Herein, we focus on how allergens induce the innate type 2 immune responses that precede activation of type 2 adaptive immunity.

Results

Allergen-induced intracellular IL-33 maturation and release

To study how allergens initiate type 2 inflammation, we tested the effect of allergen exposure on endogenous intracellular precursor IL-33 (p IL-33) moieties. We treated epithelial cells (EPC2 cells), which express endogenous IL-33, with a diverse set of allergens (Figure 1A). We employed TLR3 and TLR2 agonists, Poly (I:C) and lipopolysaccharide (LPS), as controls to mimic host epithelial barrier breach (double-stranded RNA¹⁷) and pathogen-derived endotoxins (LPS¹⁸), respectively. We found that *A. alternata*, house dust mites (HDM), *A. fumigatus*, cat dander, canary feathers, and cockroach extracts and Poly(I:C), but not birch pollen, Bermuda grass, peanut, whole wheat nor cow milk extracts, induce intracellular p IL-33 cleavage and the appearance of a shorter 21-kDa mature form of IL-33 (m IL-33) (total cell lysates; Figure 1A).

Multiple allergens triggering intracellular IL-33 maturation was unexpected because IL-33 maturation has previously been attributed to extracellular allergen-associated proteolytic activity.⁹ Thus, we aimed to elucidate the proteolytic pathway involved and examined whether IL-33 maturation was dependent upon activation of endogenous intracellular proteases. We employed selective pan-caspase (Q-VD-OPH), calpain (PD151746) and cysteine protease (E64D) inhibitors to assess the effect of IL-33 proteolytic activity on the appearance of m IL-33 moieties (Figure 1B). We also used actinomycin D to examine whether IL-33 cleavage depends on new transcription initiated by upstream signaling (Figure 1B). We found that the pan-caspase inhibitor (Q-VD-OPH) completely blocked IL-33 cleavage (Figure 1B–C), whereas neither inhibiting calpains and cysteine proteases nor halting transcription activity affected IL-33 processing. We next investigated the specific caspase(s) responsible for intracellular IL-33 cleavage. Specific inhibitors of caspases 8 (Z-IETD-FMK) and 3 and 7 (Z-DEVD-FMK; Extended Figure 1A), but not caspase 1 (Ac-YVAD-CHO; Extended Figure 1B), blocked IL-33 intracellular maturation. Conversely, allergen exposure induced activation of caspase 8 (Figure 1D) and the downstream caspases 3 and 7.

Allergen-induced activation of the effector caspase 3 and cleavage of PARP¹⁹, a caspase 3 and 7 target, were blocked with a pan-caspase inhibitor (Figure 1E–F). These data suggest that upstream caspase 8 is not only directly involved in IL-33 intracellular cleavage, but also required for caspase 3 and 7 activation and subsequent cleavage of its targets (IL-33, PARP) in a dose-dependent manner.

Ripoptosome-mediated IL-33 maturation and release

As several upstream signals can lead to formation of RIPK1-pro-caspase 8 ripoptosome complex formation, RIPK1 phosphorylation and caspase 8 activation²⁰, we examined RIPK1 involvement in driving caspase 8-dependent cleavage of IL-33. *A. alternata*, HDM, and *A. fumigatus* allergens induced rapid RIPK1 phosphorylation (p RIPK1) within 2 hours of exposure (Figure 1G); this effect was even more evident at 8 hours (Figure 1H), concurrent with IL-33 cleavage (Figure 1A), caspase 3 activation and PARP cleavage (Figure 1E). RIPK1 was rapidly cleaved in a caspase-dependent manner, as RIP phosphorylation was

detectable only in the presence of Q-VD-OPH (Extended Figure 1C). Accordingly, after 8 hours of stimulation, the necrotic cell damage-associated RIPK1 inhibitors necrostatin 1, 1s and 5 and the necroptosis inhibitor necrostatin 7 had no effect on IL-33 intracellular maturation (Extended Figure 1D). Furthermore, exogenous allergen-associated proteolytic activity was not required for allergen-induced intracellular IL-33 maturation (Extended Figure 1E). Cell viability was modestly decreased (e.g., <10% LDH release vs. mock) following allergen challenge (Extended Figure 1F), despite strong IL-33 release (Extended Figure 1G) in a dose-dependent manner. Cell damage-associated TLR3 activation was not required for allergen-induced IL-33 maturation (Extended Figure 1H).

To assess whether the identified pathway was operational in other cells, we tested skin-derived squamous epithelial cells, bronchial epithelial cells and fibroblasts. We found that IL-33 cleavage associated with caspase 8 and caspase 3 and 7 activation and PARP cleavage in diverse epithelial cells but not in fibroblasts (Extended Figure 1I), thus highlighting the proximal sensing ability of epithelial cells. We subsequently tested whether the same mechanism would trigger release of the pre-formed intracellular $mIL-33$. Indeed, IL-33 was rapidly released following stimulation with *A. alternata*, HDM and *A. fumigatus* in a dose-dependent manner; poly(I:C) served as a positive control (Figure 1I–J). In line with our previous findings, IL-33 release was effectively and specifically blocked with a pan-caspase inhibitor but not a cysteine protease inhibitor (Figure 1K).

These collective results demonstrated that intracellular $pIL-33$ processing (Figure 1A) and $mIL-33$ release (Figure 1I–K) require caspase 8 activation (Figure 1D; Extended Figure 1A), RIPK1 phosphorylation and degradation (Figure 1G–H; Extended Figure 1C) and downstream caspase 3 and caspase 7 activation (Figure 1E–F; Extended Figure 1A, E, and D). These data indicate that multiple allergens trigger a convergent pathway that involves RIPK1 phosphorylation and caspase 8 activation and results in IL-33 intracellular processing, maturation, and release. Furthermore, IL-33 maturation and release are launched by a RIPK1-caspase 8 ripoptosome-dependent activation mechanism^{20, 21} following exposure of diverse epithelial cell types to allergic stimuli.

Caspases 3 and 7 generate ST2-interacting $mIL-33$ forms

We investigated whether $pIL-33$ was directly cleaved by caspases 3 and 7 to generate $mIL-33$. Recombinant, human full-length $pIL-33$ (1–270) was incubated with recombinant, human active caspases 3, 7 and 8 (Figure 2A). $pIL-33$ was cleaved in a dose-dependent manner by either caspase 3 or 7 but not caspase 8 (Figure 2A). We examined $pIL-33$ moieties in $pIL-33$ -overexpressing epithelial cells that contain endogenous pro-caspases (Figure 2B). Adding recombinant, active caspase 8 alone activated the endogenous effector caspase 3 and led to $mIL-33$ and PARP cleavage (Figure 2B). Adding recombinant, active, effector caspases 3 and 7 resulted in endogenous caspase 3 and 7 activation in a reciprocal manner, which also produced $mIL-33$ and PARP cleavage. As a positive control, TLR3 engagement with agonist Poly (I:C) induced cleavage of endogenous PARP, caspase 3 and caspase 7 (Figure 2B). These results are consistent with caspase 8-mediated activation of effector caspase 3, which in turn cleaves and activates caspase 7. Both activated caspases 3 and 7 then cleave $pIL-33$ to generate $mIL-33$.

Caspases 3 and 7 cleave pIL-33 at residues D175 and D178

We employed mass spectrometry matrix-assisted laser desorption/ionization–time of flight (MALDI-TOF) and tandem nano-liquid chromatography mass spectrometry (nano-LCMS) to elucidate the putative caspase 3 and 7 cleavage sites of pIL-33 and mIL-33 (Extended Figure 2). We examined the pIL-33 and mIL-33 protein preparations (Figure 2A) and compared the resulting peptides profiles with known IL-33 protein sequence (Extended Figure 2A, 2B). Two distinct cleavage sites for both caspase 3 (Extended Figure 2D, G, I) and caspase 7 (Extended Figure 2F, H, J) at positions D175 and D178 were identified; these cleaved positions generated mIL-33 forms M1-D175 (1–175) and M1-D178 (1–178), respectively (Extended Figure 2C–F). The relative intensity of terminal peptide profiles further demonstrated that the human pIL-33 D178 position was preferred for caspase 3 but not caspase 7 (Extended Fig. 2G–J). These collective data demonstrate that cleaving human pIL-33 generates two mIL-33 forms ending at D175 or D178.

To characterize the biological functions of the mIL-33 forms, we examined recombinant IL-33 engineered to contain point mutations at the caspase cleavage sites. The pIL-33 (1–270), mIL-33 forms 1–175 and 1–178, and pIL-33 with point mutations (aspartate [D] to asparagine [N]) at the caspase cleavage sites at D175 (D175N), D178 (D178N), or both (D175/178N) were expressed at comparable levels (Figure 2C). We subsequently incubated cell necrotic supernatants, containing endogenous cellular components including IL-33 (see Methods), with recombinant, active human caspases 3 and 7 (Figure 2C). Both caspase 3 and 7 showed attenuated cleavage of D175N and no detectable cleavage of D178N and D175/178N. These results substantiate the mass spectrometry analysis (Extended Figure 2) by demonstrating cleavage sites that are directly targeted by caspases 3 and 7 at the residues D175 and D178.

mIL-33 forms are active with the cognate IL-33 receptor ST2

The experimentally resolved 3D structure of the human IL-33 (S117-S268)–ST2 complex was retrieved from the Protein Databank (PDB ID: 4KC3; X-ray-based) and superimposed with the nuclear magnetic resonance (NMR)-based structure of IL-33 (PDB ID: 2KLL; S111-T270) to fill in the missing loops and illustrate the residue location of D175 and D178. The structural alignment showed the means of interaction of human IL-33 with its receptor ST2 and the caspase cleavage sites (Figure 2D–E). The minimal binding domain interacting with ST2 was resolved by X-ray and NMR (S111-D175; yellow); this demonstrated that the flexible loop, containing residues D175 and D178, and the C-terminal fragment G179-T270 (grey) were posterior to the IL-33–ST2 binding interface S111-D175 (yellow) and thus were not interacting with ST2. Collectively, these data suggest that the IL-33 minimal ST2 binding domain is contained within the S111-D175 portion of the IL-1 superfamily domain S111-T270.^{22, 23}

To test the *in silico* data and assess ST2 interaction with endogenous pIL-33 and mIL-33 forms, we performed coimmunoprecipitation of IL-33 with ST2-Fc chimeric protein. Following TLR3 agonist (Poly(I:C)) stimulation (Figure 2F) and cell lysis, pIL-33 and mIL-33 were immunoprecipitated by ST2-Fc but not by control IgG. Although pIL-33 was the dominant IL-33 form, input control (whole lysate) and ST2-Fc-precipitated

IL-33 fractions contained a similar ratio of pIL-33 to mIL-33; thus, mIL-33 was precipitated as efficiently as pIL-33 and retained its ST2 binding capacity. These collective data demonstrate that the caspase-generated mIL-33 forms (M1-D175, M1-D178) retain functional ST2 binding, consistent with retaining the minimal ST2 binding domain after caspase cleavage.

ST2-specific bioactivity of mIL-33

We examined the bioactivity of mIL-33 forms using a bioassay with the ST2⁺ human mast cell line HMC-I; these cells release IL-8 when stimulated with IL-33.²⁴ We assessed IL-33 moieties generated by epithelial cells (TE-7) following cellular transduction; these cells were engineered to express mIL-33 forms and the pIL-33 WT with cleavage-site point-mutations at comparable levels (Figure 3A). We employed ST2⁺ HMC-I reporter cells²⁴ to assay ST2-specific activity in cellular necrotic supernatants containing IL-33 forms (see Methods; Figure 3B–C). Notably, the bioactivity of cellular supernatants of mIL-33-expressing cells was significantly higher than that of pIL-33-expressing cells and comparable to that of mIL-33-containing cells pre-treated with TLR3 agonist (Figure 3B). Importantly, point mutations in the flexible loop domain (Figure 2C) did not have a significant effect on the IL-33 bioactivity (vs. pIL-33; Figure 3C). IL-8 release was significantly reduced by blocking with anti-ST2 antibody (Figure 3B–C), demonstrating specific measurement of IL-33-induced bioactivity in HMC-I cells.

To further assess mIL-33 bioactivity, we produced cell-free recombinant forms of pIL-33 (1–270), mIL-33 1–175, and mIL-33 1–178 forms (see Methods). Recombinant proteins were normalized to equimolar quantities (Figure 3D), and bioactivity was assessed using the ST2⁺ HMC-I reporter cells. Both mIL-33 forms had higher bioactivity than did pIL-33 (1–270); specificity was asserted by blocking with anti-ST2 antibody (Figure 3E). We tested the activity of the IL-33 forms on primary murine eosinophils²⁵ focused on the release of IL-6, CXCL2 and IL-4 (Figure 3F–H). mIL-33 forms triggered higher responses than did pIL-33, and responses were reduced by anti-ST2 antibody (Figure 3F–H).

To substantiate the *in vivo* relevance of these findings, wheat germ-produced pIL-33 and mIL-33 were intraperitoneally injected into mice at equimolar quantities (10 nM). We employed IL-33-deficient (knockout [KO]) mice to exclude possible effects of endogenous IL-33, as IL-33 induced intraperitoneal macrophage activation and neutrophil recruitment in mice,²⁶ and assessed IL-33 effects on distinct inflammatory macrophages and neutrophil populations by flow cytometry (Extended Figure 3A–B). mIL-33 forms elicited higher influx of inflammatory macrophages (Extended Figure 3B–C) and neutrophils (Extended Figure 3B, D) than did pIL-33. We therefore conclude that IL-33 induces consistent proinflammatory and pro-type 2 responses and that mIL-33 are the bioactive species of IL-33.

Histone co-release and mIL-33 bioactivity potentiation

The mIL-33 1–175 and 1–178 forms include the minimal ST2 binding domain and the N-terminal fragment M1–110D, containing the intact IL-33 chromatin-binding domain M44–58C²⁴ (Figure 2D–E). pIL-33 is co-released with histones following cellular necrosis; this

co-release potentiates its bioactivity.²⁴ We hypothesized that $mIL-33$ is co-released with histones following ripoptosome activation and that co-release enhances $mIL-33$ bioactivity. Increasing concentrations of secreted $mIL-33$ were observed in the culture medium of TLR3 agonist-treated cells in a kinetic fashion over 24 hours (Extended Figure 4A–B; released fraction). Immunoblot analyses showed that secreted $mIL-33$ (Extended Figure 4B; released fraction) was proportional to the generation of intracellular $mIL-33$ (Extended Figure 4B; cellular fraction). We analyzed the medium containing the secreted $mIL-33$ (released fraction) using size exclusion chromatography (Extended Figure 4C–E). A UV absorption plot of the eluted fractions (280 nm for proteins; Extended Figure 4C) and immunoblot analysis demonstrated that IL-33 and histones were present in the same fractions (Extended Figure 4D). The molecular weight of the protein complexes was determined by comparing their elution fraction (1 to 95) to a standard curve (fraction MW; Extended Figure 4E). The $mIL-33$ forms were secreted as heteromeric complexes in the same large-molecular-weight fractions that were rich in histones (>100 kDa, fractions 35–67). $mIL-33$ forms and histones were also found in separate homogenous, low-molecular-weight fractions (~30 kDa, fractions 69–77; ~20 kDa, fractions 78–85) (Extended Figure 4C–E).

To assess whether histones could potentiate $mIL-33$ activity, we treated HMC-I cells with various IL-33 proteins in the presence and absence of purified histones (as described elsewhere²⁴). ST2-specific bioactivity was examined by neutralizing with anti-ST2 blocking or control antibody (Extended Figure 4F–G). Indeed, $pIL-33$ baseline activity was potentiated with histones, $mIL-33$ exhibited higher ST2-specific bioactivity than did $pIL-33$ and $mIL-33$ activity was potentiated in the presence of histones.

These collective data demonstrate that ripoptosome activation triggers the maturation and secretion of $mIL-33$ and histones complexes and that histones can potentiate $mIL-33$ bioactivity.

Caspase 8 inhibition attenuates allergic airway inflammation

To evaluate the caspase 8-rioptosome activation pathway in the development of allergic inflammation *in vivo*, we induced allergic airway inflammation in a murine model by repeated challenge with *A. alternata* in the presence of the caspase 8-specific inhibitor Z-IETD-FMK (Figure 4). Analyzing released IL-33 in bronchoalveolar lavage fluid (BALF) showed that *A. alternata* induced marked release of $mIL-33$, but not $pIL-33$, and that this release was completely abrogated by the caspase 8 inhibitor (Figure 4 A–B). *A. alternata* induced a ~4-fold increase in total BALF cell counts in WT mice (Figure 4D) and marked influxes of neutrophils (Figure 4E) and eosinophils (Figure 4F), which were significantly abrogated by caspase 8 inhibition (Figure 4D–F) (flow cytometry cell gating strategy in Extended Figure 5A). As a control for IL-33-mediated effects, we used IL-33-deficient (KO) mice; they had no detectable, secreted IL-33 under any condition (Figure 4C). IL-33 KO mice challenged with *A. alternata* developed ~2-fold increase in total BALF cell counts (Figure 4G) and modest influxes of neutrophils (Figure 4H) and eosinophils (Figure 4I), which were significantly lower than that of WT counterparts and unaffected by caspase 8 inhibition (Figure 4G–I). We assessed the level of type 2-associated cytokines IL-4, IL-5, IL-6, IL-13 and eotaxin in BALF of WT and IL-33 KO mice (Extended Figure

5B–C) challenged with *A. alternata* and treated with a caspase 8–specific inhibitor. WT mice developed potent type 2 cytokine responses, which were inhibited with Z-IETD-FMK (Extended Figure 5B). IL-33 KO mice showed modest responses (Extended Figure 5C) that were lower than those of WT counterparts and unaffected by caspase 8 inhibition.

To further substantiate the role of epithelial cell caspase 8-ripiptosome activation in mediating allergic responses, we examined allergen-induced airway inflammation in mice with targeted deletion of caspase 8 in bronchial epithelial cells by generating CC10-CreER^{+/−}/Casp8^{fl/fl} mice (caspase 8 KO; see Methods). Allergic airway inflammation was induced by repeated challenge with *A. alternata* (Figure 5). *A. alternata* induced marked release of _mIL-33, but not _pIL-33, in WT mice (Figure 5A–B). Caspase 8 KO mice had attenuated _mIL-33 secretion (Figure 5A–B). Furthermore, caspase 8–deficient mice had ~3-fold lower total BALF cell counts (Figure 5C) and lower neutrophil and eosinophil levels (Figure 5D–E) than did WT counterparts (flow cytometry cell gating strategy in Extended Figure 6A). We assessed the type 2 inflammation–associated cytokines IL-4, IL-5, IL-6 and IL-13 and eosinophil-specific chemokine eotaxin 1 in BALF of WT and caspase 8 KO mice (Extended Figure 6B) challenged with *A. alternata*; caspase 8 KO mice showed modest or non-significant responses that were lower than those of WT counterparts.

We assessed active caspase 8 and IL-33 expression in bronchial epithelial cells of the caspase 8 KO and control mice challenged with *A. alternata* (Extended Figure 7). As expected, caspase 8 KO mice challenged with *A. alternata* did not stain positively for active caspase 8, whereas IL-33 expression was detected similarly under all conditions (Extended Figure 7A). Quantitative analysis demonstrated that *A. alternata* markedly increased active caspase 8 expression in WT but not caspase 8 KO mice (Extended Figure 7B). IL-33 staining was not significantly affected by *A. alternata* treatment; however, a lower percentage of epithelial cells (percent affected area) stained positively for IL-33 in caspase 8 KO mice (Extended Figure 7C). Thus, these findings suggest that significantly less IL-33 was being actively secreted in caspase 8 KO mice (consistent with Figure 5A–B). Furthermore, IL-33 staining in the cytoplasm of epithelial cells strongly correlated with active caspase 8 expression in WT mice, but showed a low correlation in caspase 8 KO mice (Extended Figure 7D–E).

Thus, using two independent in vivo approaches (pharmacologic inhibition, gene deletion), we have substantiated that the caspase 8-ripiptosome mediates allergic airway responses by regulating _mIL-33 secretion and the innate type 2 inflammatory cellular response, including neutrophilia and eosinophilia.

Riptionsome activation in human allergic inflammation

To test the clinical significance of our findings, we chose to examine the human allergic disease eosinophilic esophagitis (EoE) due to its association with type 2 inflammation,²⁴ including dynamic expression of IL-33.²⁷ The ready availability of esophageal biopsies allowed us a unique opportunity to probe human allergic inflammation at the tissue level. Esophageal biopsies from patients with active EoE demonstrated increased expression of active caspase 8 (Figure 6A–B) and a greater number of caspase 3 positive cells (Figure 6A, C); these two parameters correlated with each other (Figure 6D). As expected, biopsies from

active EoE showed higher eosinophilia than did biopsies from control individuals or patients with EoE in remission (Figure 6A, E). Interestingly, both ripoptosome activation markers—active caspase 8 and active caspase 3 staining—strongly correlated with esophageal eosinophilia (Figure 6F–G). Furthermore, mIL-33 expression (Figure 6H–I) was increased in patients with active EoE compared with control individuals and patients with EoE in remission (Figure 6I). mIL-33 expression positively correlated with active caspase 8 and active caspase 3 staining levels in epithelial cells (Figure 6J–K) and the degree of eosinophilia (Figure 6L). These collective data demonstrate that the activation of in situ ripoptosome activation markers caspase 8 and caspase 3 and generation and maturation of pIL-33 are associated with human allergic eosinophilic inflammation.

Discussion

Herein we define an unexpected set of intracellular signaling events triggered by a broad array of environmental allergens, including fungi, insects and mites. We demonstrate that allergens trigger ripoptosome activation as evident from rapid RIPK1 phosphorylation and pro-caspase 8 activation. Subsequently, active caspase 8 degrades RIPK1 (thus inhibiting necroptosis) and activates effector pro-caspases 3 and 7, which directly process pIL-33 into an active form that is subsequently released; we refer to this newly identified pathway as “RipIL-33” (Extended Figure 8). Ripoptosome-mediated release of IL-33 preceded substantial release of LDH. Thus, RipIL-33 allergen sensing is a pre-programmed imminent sequence of molecular events beginning with ripoptosome activation and preceding cell death. Notably, caspase 8 activation may occur by intra- and interdimeric self-cleavage,²⁸ resulting in differential generation of mIL-33 moieties also independent of necroptosis²⁹ (as assessed with necrostatins), proteolytic tissue damage⁹ and the protease-activated receptor (PAR) pathway³⁰ (as assessed with protease inhibitors). RipIL-33 pathway is present in diverse epithelial cell types, consistent with the epithelium forming the first line of defense against environmental stimuli and thus likely having evolved to sense diverse, antigenic stimuli to initiate type 2 responses.

Notably, allergens comprise heterogeneous constituents, including bioactive PAMPs that can be sensed by various PRRs. Indeed, PAMP sensing by PRR and PRR dysregulation have been associated with atopy.^{2, 7, 31} Although pattern recognition has a well-established role in myeloid cells⁴, there is a lack of clarity on whether canonical PRR signaling is functional in epithelial cells. Our data indicate that although TLR3 can induce ripoptosome activation, the allergen-sensing mechanism is independent of TLR3 PRR. However, multiple, upstream, PAMP- and DAMP-induced signals may converge to activate an intracellular system in epithelial cells that releases the bioactive IL-33 alarmin and initiates the allergic arm of immunity. Importantly, allergic inflammation can be associated with atopic or non-atopic diseases. In atopy, the adaptive IgE-mediated responses can be immediately triggered but are also amplified in an IL-33-mediated manner.^{32, 33} We thus propose that the RIPK1-caspase 8 ripoptosome complex is an epithelial cell, allergen-sensing platform that detects diverse allergic stimuli, resulting in caspase-mediated cleavage, activation and release of IL-33 alarmin. Released IL-33 elicits innate type 2 responses and amplifies adaptive responses in both atopic and non-atopic forms of allergic inflammation.^{32, 33} Pro-atopy IL-1 family alarmins (e.g., IL-18²⁹ and IL-1 β ⁴), whose activation and release are also mediated by

caspase 8^{34,4}, may also be released via this pathway. These findings define a previously unknown role of the ripoptosome and associated caspases in modulating epithelial barrier immune function^{35, 36} and activating and releasing IL-1 family alarmins^{4, 29, 34} to trigger type 2 immunity and allergic disease.

We demonstrated that pIL-33 cleavage preserved the ST2 minimal binding domain (S111-D175) in mIL-33 forms and maintained functional interaction with the ST2 receptor, as evident from in silico modeling, ST2/IL-33 co-immunoprecipitation and ST2 bioactivity assays. Our structural studies of IL-33/ST2–IL-1RAcP complex x-ray and NMR data further revealed that the 179–270 C-terminal residues have limited or no interaction with ST2 and the IL-1RAcP complex.^{22, 23, 37} Notably, the chromatin binding domain (M1-S110) of IL-33 is also retained in mIL-33 forms; we show that mIL-33 was released in complex with histones, which enhanced mIL-33 bioactivity.²⁴ The proposed model accommodates the possibility that pIL-33 can be released and processed extracellularly by other proteases; notably, pIL-33 can induce atypical non-type 2 airway inflammation.³⁸ However, the allergen-induced release of pIL-33 has been proposed to occur only within minutes after the allergen-induced injury and then decline to undetectable levels within one hour.⁹ In contrast, ripoptosome activation triggers secretion of mIL-33 moieties over a sustained period of time and mIL-33 generation was proportional to secreted mIL-33. In contrast, intracellular pIL-33 gradually declined, and wasn't extracellularly detected.

Previous studies suggested extracellular IL-33 activation by neutrophils and mast cell-derived proteases.³⁹ Yet, this paradigm does not explain how allergens are sensed or how they prime and maintain type 2 responses. Indeed, immune cell influx has been shown to mainly occur in response to IL-33 secretion and not preceding it.^{9, 12, 13, 26, 39} Furthermore, extracellular pIL-33 processing yields short-lived mIL-33 forms, generating greater fraction of degraded IL-33 moieties. Indeed, the same proteases that generate mIL-33 rapidly degrade it, particularly at ST2-binding domain.⁴⁰ Herein, we showed that intracellular cleavage by caspases is highly specific and generates stable IL-33 forms as compared with extracellular non-specific digestion by exogenous serine proteases.³⁹ Furthermore, our findings are consistent with data concerning other IL-1 superfamily cytokines, which are activated by caspases²⁹, including original reports focused on caspase-mediated enhancement of IL-33 physiologic activity.^{16, 41, 42, 43, 44}

A variety of pre-clinical and clinical investigations indicated that the IL-33/ST2 axis is a potent pro-atopy pathway.⁴⁵ As such, posttranslational modifications of IL-33, leading to its activation and/or inactivation, can have profound effects on type 2 immune responses.^{8, 12, 46} Herein, we present evidence for the ripoptosome pathway being involved in murine and human allergic inflammation. In particular, caspase 8 inhibition attenuated the IL-33/ST2 axis-dependent type 2 cytokines and influx and activation of innate immune cells (e.g., neutrophils, eosinophils). We substantiate caspase 8 involvement by demonstrating attenuation of allergen-induced IL-33 release and lung type 2 inflammation in mice by Scgb1a1/Cc10-targeted *caspase 8* deletion in bronchial epithelial cells.⁴⁷ Notably, IL-33 is also expressed in type 2 pneumocytes^{13, 48}, thus accounting for complete abrogation of allergen-induced IL-33 release in mice treated with the caspase 8-specific inhibitor Z-IETD-FMK compared to mice with Scgb1a1/Cc10-targeted *caspase 8* deletion in bronchial

epithelial cells alone. Notably, active caspase 8 expression strongly correlated with IL-33 secretion in these models. Human clinical data further validate ripoptosome-mediated IL-33 maturation as contributing to eosinophilic inflammation in the human allergic disease EoE; we found that ripoptosome activation markers and mature IL-33 levels dynamically correlated with the degree of esophageal eosinophilia and disease activity. These findings are in line with the reported caspase-mediated cleavage of the KRT18 and DSG1 structural proteins in EoE.^{36, 49}

In summary, we have identified an epithelial barrier, allergen-sensing mechanism that converges on the ripoptosome as an intracellular molecular signaling platform triggering type 2 innate immune responses, referred to as RipIL-33. Furthermore, we provide evidence for the clinical and therapeutic significance of the RipIL-33 allergen sensing pathway. We therefore propose that disrupting caspase 8-rioptosome activation provides a unique potential entry point to counteract type 2 immunity and alleviate allergic inflammation.

Materials and Methods

Cell culture and selective inhibitors

The TE-7 human esophageal epithelial cell line (gift from Pierre Hainault, PhD, International Agency for Research on Cancer, Lyon, France) and HMC-I human mast cell line (EMD Millipore) were cultured in RPMI-1640 medium (Invitrogen) supplemented with 5% fetal bovine serum (FBS).

HBEC3-KT cells (ATCC) are CDK4- and hTERT-immortalized normal human bronchial epithelial cells; HaCaT is an immortalized keratinocyte cell line from adult human skin (gift from Dr. T. Bowden, University of Arizona, Tucson, AZ); EPC2 cells from an hTERT-immortalized normal human esophageal epithelial cell line (gift from Anil Rustgi, PhD, University of Pennsylvania, Philadelphia, Pennsylvania, USA) and primary esophageal epithelial cells were cultured in keratinocyte serum-free media (KSFM; Life Technologies). In all experiments, these cells were maintained as a super-confluent monolayer (1×10^6 cells/cm²) to induce organotypic epithelial barrier formation and support endogenous IL-33 expression.

The HEK293T human embryonic kidney cell line (ATCC) and FEF3 primary fetal esophageal fibroblasts (gift from Hiroshi Nakagawa, MD, PhD, University of Pennsylvania, Philadelphia, Pennsylvania, USA) were maintained in Dulbecco's Minimum Essential Media (DMEM) supplemented with 10% FBS (Gibco)

In all experiments, the cells were co-incubated with cell-permeable proteasome inhibitor MG-132 (CAS 133407-82-6; Calbiochem) at a final concentration of 5 μ M in the medium in order to improve post-translational modifications visualization by immunoblotting as described elsewhere.⁵⁰ The following cell-permeable inhibitors were used as indicated: irreversible inhibitor of cysteine proteases E64D (CAS 88321-09-9; Calbiochem), selective calpain inhibitor PD151746 (CAS 179461-52-0; Calbiochem), RNA polymerase inhibitor Actinomycin D (CAS 50-76-0; Calbiochem), pan-caspase inhibitor Q-VD-OPH (OPH001-01M; R&D), caspase 8 inhibitor Z-IETD-FMK (FKM007; R&D), caspase 3

inhibitor Z-DEVD-FMK (FMK004; R&D), caspase 1 inhibitor Ac-YVAD-CHO (10016; Cayman), Necrostatin-1 Inactive Control (21192; Cayman), Necrostatin 1 (11658; Cayman), Necrostatin 5 (10527; Cayman), Necrostatin 7 (10528; Cayman), and Necrostatin 1s (17802; Cell Signaling).

cOmplete EDTA-free protease inhibitors cocktail (PIC; 4693159001; Roche) was immediately added to cells supernatants at the harvest for the follow up analyses.

Cell viability was assessed in CyQUANT LDH cytotoxicity assay (C20300; Invitrogen).

All cell lines were authenticated and confirmed to be mycoplasma free in compliance with NIH guidelines. For the complete details on cell lines, Mycoplasma testing and cell line validation please refer to Supplemental Information file. Cell cultures were maintained at 37°C in a humidified 5% CO₂ incubator.

Generation of CRISPR/Cas9 *TLR3* knockout EPC2 cells

A guide RNA (gRNA) complementary to the *TLR3* open reading frame sequence and located directly 5' of a protospacer adjacent motif (PAM) was identified (gRNA: 5' - CTACATCCAAGCTAGTTAGC - 3'), and the following oligonucleotides (5' - CACCGTACATCCAAGCTAGTTAGC- 3' and 5' -AAACGCTAACTAGCTTGGATGTAC - 3') were annealed and ligated into the plasmid pX459M2 to produce pX459M2-*TLR3*g. EPC2 cells were transfected with pX459M2-*TLR3*g using Viromer (Cat. TT100302; Origene) according to the manufacturer's protocol. Transfected cells were selected using Puromycin (Cat. SBR00017; SIGMA) and subcloned in the presence of irradiated NIH3T3 feeder cells. Resulting EPC2 cell clones were expanded, and genomic DNA was extracted using the Quick gDNA micro prep kit (Cat. D3020; ZYMO) according to the manufacturer's protocol. For each clone, genomic DNA in the vicinity of the predicted edited region was amplified with primers 8779 (5'- ACCAAGTGCACCTGTTAGCCA -3') and 8780 (5'- G AGCTCATTGTGCTGGAGGTT-3') and sequenced with primer 8779 to assess whether editing occurred. Genomic DNA from edited clones was amplified with primers 8779 and 8780 and was cloned into pCRII-TOPO; several pCRII-TOPO clones derived from each EPC2 clone were sequenced to verify the nature of editing that occurred in each allele. Deconvolution of Sanger sequencing profiles was performed using TIDE (<https://tide.deskgen.com>) to identify the nature of the alleles present in each clone. *TLR3* knockout clones were defined as those having 2 alleles with insertions and/or deletions consisting of a quantity of nucleotides that was not a multiple of 3. Control clones were those transfected with pX459M2-*TLR3*g but not having any editing present at the *TLR3* locus. Protein expression of control and *TLR3* knockout clones was assessed by immunoblotting.

Animals

C57BL/6 and BALB/C mice were obtained from Charles River Labs and IL-33^{Cit/Cit} IL-33 KO mice were obtained from Andrew N. J. McKenzie, PhD (MRC Laboratory of Molecular Biology, Hills Road, Cambridge, UK). C57BL/6 caspase 8 targeted KO mice were generated by breeding Scgb1a1 (CC10)-CreER^{+/+} (Jackson stock No: 016225) mice with Casp8^{fl/fl} (Jackson stock No: 027002) mice to generate CC10-CreER^{+/-}/Casp8^{fl/fl} mice. Caspase 8 targeted KO was achieved by treating mice with 2mg tamoxifen in corn oil via daily gastric

gavage for 7 consecutive days beginning 5 days ahead of *A. alternata* challenge. C57BL/6 WT mice were treated with tamoxifen as well to ensure proper controlled experimental settings for *A. alternata* challenge. All the animals were maintained in accordance with the Institutional Animal Care and Use Committee (IACUC) guidelines and protocols approved by the Cincinnati Children's Hospital Medical Center (CCHMC) IACUC committee. For the complete list of animal research subjects, please refer to Supplemental Information file.

Induction of IL-33–dependent airway inflammation

IL-33–dependent airway inflammation was induced in C57BL/6, BALB/C WT and IL-33 KO and caspase 8 KO mice: briefly, mice were challenged with a daily *A. alternata* intratracheal (IT) injection (12.5 µg/mouse in phosphate-buffered saline [PBS]) for 3 consecutive days and 24 hours apart. On each day of IT challenge, BALB/C WT and IL-33 KO mice (not treated with tamoxifen) received 2 intravenous (IV) injections of 0.1% DMSO in sterile saline (Z-IETD-FMK, 10 µg/ g of mouse weight) 2 hours apart - 60 minutes before and 60 minutes after the *A. alternata* IT challenge. Mice were terminated on day 3, 4 hours after the second IV injection. IT injections and bronchoalveolar fluid (BALF) collection: briefly, mice were injected with 30 µL of agent containing saline as indicated. Mice were terminated and lungs were washed with 600 µL of saline supplemented with 1:10 solution in saline of cOmplete EDTA-free protease inhibitors cocktail (PIC; 4693159001; Roche). After the cells were removed by centrifugation, BALF was supplemented with 1:1 solution of PIC in saline. Next IL-33 concentrations were determined by ELISA (DY3626; R&D) or by immunoblotting as indicated.

Induction of IL-33 dependent intraperitoneal inflammation

IL-33 dependent intraperitoneal macrophage activation and neutrophil recruitment in mice was induced as described elsewhere ²⁶. Briefly, mice were intraperitoneally injected with wheat germ–produced pIL-33 and mIL-33 forms – see “IL-33 overexpression, secretion, and recombinant protein production” section below. After 6 hours, the mice were terminated, and peritoneal lavage was collected. Peritoneal cells were analyzed by flow cytometry – see “Flow cytometry analysis” section below.

Flow cytometry analysis

Mice were injected with 200 ng (6.5 pmol) of IL-33. After 6 hours, the peritoneum was washed once with 5 mL cold PBS. Cells were collected from the peritoneal washes and stained for 45 minutes on ice in PBS supplemented with 2% FBS. The following antibodies were used: FcR-γ–blocking antibody (anti-CD16/CD32, clone 2.4G2; BD Biosciences, 553142), PerCP-Cy5.5 anti-CD45 (clone 30-F11; eBiosciences, 45–0451), V450 anti-CD11b (clone M1/70; BD Horizon, 560455), FITC anti-CD117 c-KIT, clone 2B8; BioLegend, 105805), PE-Cy7 anti-Ly-6G/ Ly-6C (GR-1, clone RB6–8C5; BioLegend, 108415). Data were acquired on an BD LSRFortessa flow cytometer (BD Biosciences) and analyzed with FlowJo software (TreeStar, Ashland, OG). Dead cells and cell doublets were excluded. The percentage of each population was derived as described elsewhere ²⁶ and using the following markers: mast cells CD45⁺ c-KIT⁺ CD11b⁻, neutrophils CD45⁺ Ly-6G/C^{high} CD11b⁺, and inflammatory macrophages CD45⁺ Ly-6G/^{intermediate} CD11b⁺

cells. For the complete list of antibodies, dilutions and validation information please refer to Supplemental Information file.

IL-33 overexpression, secretion, and recombinant protein production

In order to generate TE-7 cells with stable, constitutive overexpression of full-length wildtype or point-mutated IL-33, the cDNA for the *Homo sapiens* full-length *IL33* mRNA (NM_033439.4) was cloned into the pINDUCER20 vector via the Gateway cloning system (Promega). Lentiviral particle production and TE-7 cell transduction were performed as previously described²⁴. Cell supernatants used to stimulate ST2 -dependent responses and in caspase cleavage arrays were necrotic supernatants (NS). NS were prepared by freeze and thaw as described elsewhere²⁴, and IL-33 equimolar normalization was performed using immunoblotting. In IL-33 secretion assays, the concentration of released IL-33 in cell culture supernatants was determined by ELISA (DY3625; R&D) as indicated.

For analyzing proteolytic maturation by mass spectrometry, full-length glutathione S-transferase (GST)-tagged recombinant human IL-33 was obtained from Abnova (Wheat Germ Extract Produced; H00090865-P01). For in vitro and in vivo IL-33 bioactivity assays, as well as for caspase cleavage arrays full-length and truncated *IL33* cDNA (NM_033439.4) were codon optimized to facilitate protein translation (NP_254274.1) and cloned into pTNT vector (L5610; Promega); the recombinant proteins were produced using the TnT Coupled Wheat Germ Extract Transcription/Translation Systems (L5030; Promega) according to the manufacturer's specifications. The resulting IL-33 proteins were qualitatively assessed using immunoblotting. IL-33 concentrations were determined by ELISA (DY3625; R&D) assays as indicated and analyzed again using immunoblotting to verify proper normalization.

Recombinant human active caspase 8 (705-C8-010), caspase 7 (823-C7-010), caspase 3 (707-C3-010), and human ST2-Fc chimeric protein (523-ST-100) were obtained from R&D. Caspase proteolytic activity was tested in accordance with the manufacturer's recommendations and in PBS supplemented with cOmplete EDTA-free protease inhibitors (4693159001; Roche).

Recombinant human TNF- α (300-01A) was obtained from Peprotech.

ST2-mediated IL-33 bioactivity assay

HMC-I human mast cells were plated in 96-well plates at 100,000 cells per well in 150 μ L of medium per well and stimulated for 8 hours with NS containing IL-33 or recombinant human IL-33 as described above and/or with acid-purified histones²⁴. The IL-8 level in supernatants was determined by IL-8 ELISA (431504; BioLegend) following the manufacturer's instructions.

Murine eosinophils were maintained as previously described.²⁵ Cytokine levels in supernatants were determined by multiplex ELISA (Eve Technologies). In some experiments, cells were treated with ST2-blocking antibody (AF523 and MAB523 for human cells and AF1004 for mouse cells; R&D) or control IgG (AB-108-C; R&D). For the complete list of antibodies, dilutions and validation information please refer to Supplemental Information file.

Environmental allergen extracts

Alternaria alternata (My1), House Dust Mites (B82), *Aspergillus fumigatus* (My3), White Birch (80), Bermuda Grass (T2), Canary Feathers (E2), Cow Milk (F395), Peanut (F171), Cat Dander (E63), American Cockroach (B26) and Whole Wheat (F235) extracts from Greer Laboratories.

PRR agonists

Pattern recognition receptor (PRR) TLR3 agonist was used to test the functional activity of TLR3 InvivoGen (Cat. No. tlrs-arr; Poly(I:C) HMW).

Mass spectrometry and tandem liquid chromatography

Coomassie gel samples of caspase 3- and caspase 7-cleaved, GST-tagged, full-length IL-33 protein was reduced with dithiothreitol (DTT), alkylated with iodoacetamide (IAA), and digested with chymotrypsin. The peptides were extracted, dried by speed vac evaporator, resuspended in 12.5 μ L of 0.1% formic acid (FA), and 80% desalted using micro C18 zip tips (Z719994; Millipore). The samples were mixed with an alpha cyan-4-hydroxy cinnamic acid (HCCA) matrix and spotted for analysis by MALDI-TOF and concurrently run by nano-LCMS on a SCIEX 5600. Chymotryptic peptides confirming the GST and IL-33 sequence coverage and fragmentation patterns were obtained and aligned with existing IL-33 sequence (NP_254274.1).

Immunoblotting

Total cell lysates were obtained from cells lysed with RIPA lysis buffer (89900; ThermoFisher) supplemented with LDS sample buffer (NP0007; Invitrogen), 5% 2-mercaptoethanol (21985023; Gibco), cOmplete EDTA-free protease inhibitors (4693159001; Roche), phosSTOP phosphatase inhibitors (94906845001; Roche), and pan-caspase inhibitor Q-VD-OPH (OPH001-01M; R&D).

Following standard immunoblotting, membranes were blocked with Odyssey blocking buffer (927-50000; LiCOR) and probed with the following antibodies: goat anti-human IL-33 (AF3625; R&D), goat anti-mouse IL-33 (AF3626; R&D), rabbit anti-total histone H3 (ab1791; Abcam), mouse anti-histone H2B (ab52484; Abcam), mouse anti-HSP90 (TA500494; Origene), mouse anti-GAPDH (2D9; Origene), rabbit anti-caspase 8 (AF1650; R&D), rabbit anti-cleaved caspase 3 (9664; Cell Signaling), rabbit anti-cleaved caspase 7 (8438; Cell Signaling), rabbit anti-PARP (9542; Cell Signaling), rabbit anti-RIP (3493; Cell Signaling), rabbit anti-phosphorylated RIP (65746; Cell Signaling), and goat anti-human TLR3 (AF1487; R&D). The secondary infrared dye (AF680 and AF790)-conjugated donkey anti-IgG (H+L) and minimal cross-reactivity (705-625-147; 705-655-147; 715-625-150; 715-655-150; 711-625-152; 711-655-152) antibodies were obtained from Jackson ImmunoResearch. For the complete list of antibodies, dilutions and validation information please refer to Supplemental Information file. Membranes were imaged on an Odyssey IR imager with Image Studio software (Li-COR). All the immunoblot scanned uncropped full images are presented in the Fig. 1-6 and Extended Data Fig. 1-7.

Co-immunoprecipitation

Protein concentrations were determined by bincinchonic acid (BCA) assay (23227; Thermo Scientific). Equal amounts of protein lysate were precleared for 2 hours at 4°C with Protein A/G beads (sc-2003; Santa Cruz) in the presence of 250 mM NaCl, 1% NP-40, 1 mM EDTA, and protease inhibitors. Samples were incubated overnight at 4°C with 2 µg of chimeric ST2-Fc protein. Samples were incubated for 1 hour at 4°C with Protein A/G beads before elution with glycine (pH 2.8). Protein expression in eluates was determined by immunoblotting as described above.

Size exclusion chromatography

TE-7 cells were stimulated in OPTI-MEM serum-free medium (31985062; Gibco), and supernatant samples were collected. Samples were treated with DNase (10104159001; Roche) and concentrated using 10-kDa Amicon Ultra-0.5 mL Centrifugal Filters (UFC501096; Millipore). Size exclusion chromatography was run on supernatants using a GE Healthcare HiPrep 16/60 Sephacryl S-100 HR column (GE17-1165-01; GE). The protein concentration was continuously monitored by measuring UV absorbance at a wavelength of 280 nm. Fractions of 1 mL were collected. Fractions were concentrated as described above, and the protein expression in eluates was determined by immunoblotting as described above.

Protein structure analysis

Experimentally resolved structures of human IL-33 and ST2 were retrieved from the Protein Databank (PDB). Because the crystal structure of the ST2 receptor and IL-33 complex (PDB ID: 4kc3) does not contain the flexible loops of IL-33, an additional solution NMR-based structure was retrieved (PDB ID: 2kl1) and superimposed with the X ray-based counterpart to fill in the loops and illustrate the location of positions D175 and D178. The N-terminal portion of endogenous IL-33, containing the chromatin-binding domain (M1-H109), was not modeled as no homologous structure template was available at the time of modeling. The protein structure alignment, analysis, and visualization were performed using PyMol.

Procurement and processing of esophageal biopsies and immunohistochemistry

This study was performed with the approval of the CCHMC Institutional Review Board. Informed consent was obtained from patients or their legal guardians to donate tissue samples for research and to have their clinical information entered into the Cincinnati Center for Eosinophilic Disorders (CCED) database. Patients were 4 to 17 years old, 13 males and 3 females. Patients with active EoE were defined as those having 15 or more esophageal eosinophils per high-power microscopic field at the time of biopsy and not receiving swallowed glucocorticoid or dietary treatment at time of endoscopy. Esophageal biopsies and murine tissues were fixed with formalin and embedded in paraffin (FFPE). Antigen retrieval, H&E, MBP, IL-33, active caspase 8 and caspase 3 staining were performed as described elsewhere.³⁶ Images were analyzed with ImageJ (Fiji open-source Java image processing program).

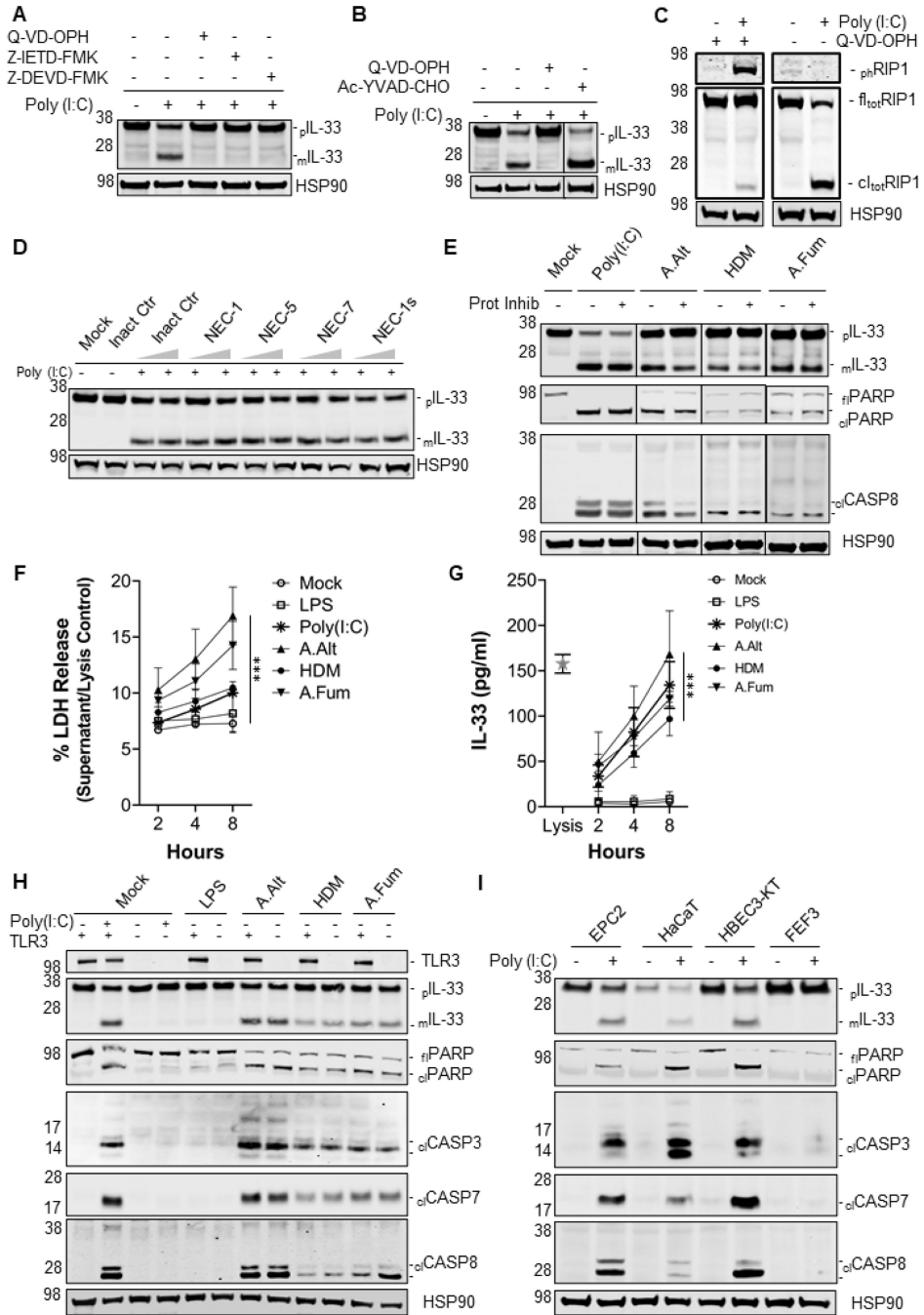
Statistical analysis

GraphPad Prism software was used for the indicated statistical analyses. A P value ≤ 0.05 was considered statistically significant.

Data Availability Statement

No accession codes, unique identifiers, or web links for publicly available datasets were generated or required for this publication. Main and extended figures have associated immunoblot scans that are presented in the Source Data Set 1. All figures have associated raw data. The additional data that support the findings of this study are available from the corresponding author upon request.

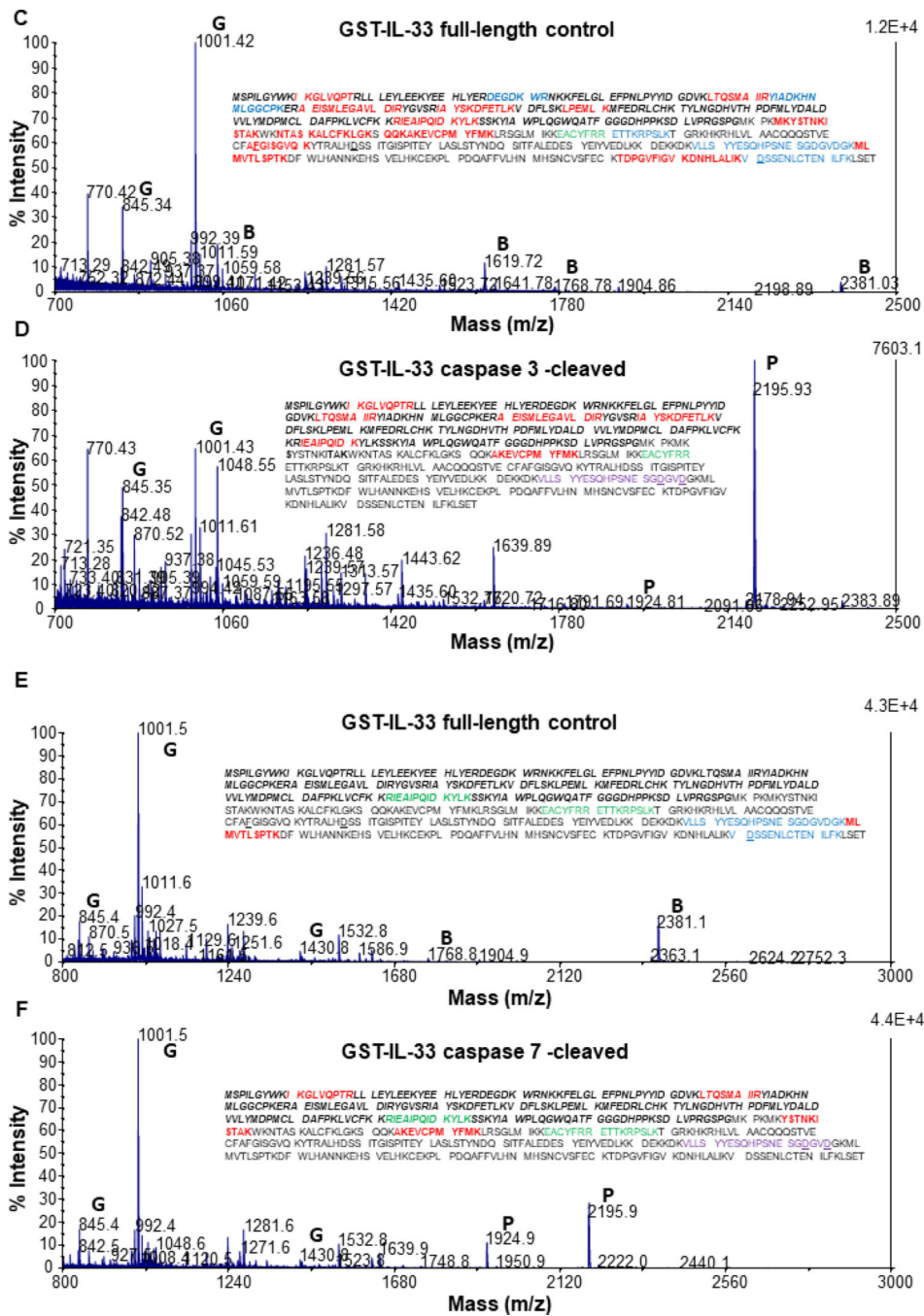
Extended Data



Extended Data Fig. 1. Ripoptosome-dependent intracellular pIL-33 maturation

A-E. Immunoblot analysis of intracellular IL-33 and cellular components from total cell lysates of cells expressing endogenous pIL-33 and exposed to various stimuli. EPC2 cells were treated for 8 hours with control medium alone (Mock), 10 nM of Poly (I:C) or LPS, or 25 µg/mL of A. alternata (A.Alt), house dust mite (HDM), or A. fumigatus (A.Fum) allergen extracts as indicated. EPC2 cells were treated in the presence of control medium (Mock) or in the presence of 20 µM pan-caspase inhibitor (Q-VD-OPH), caspase 8 inhibitor (Z-IETD-

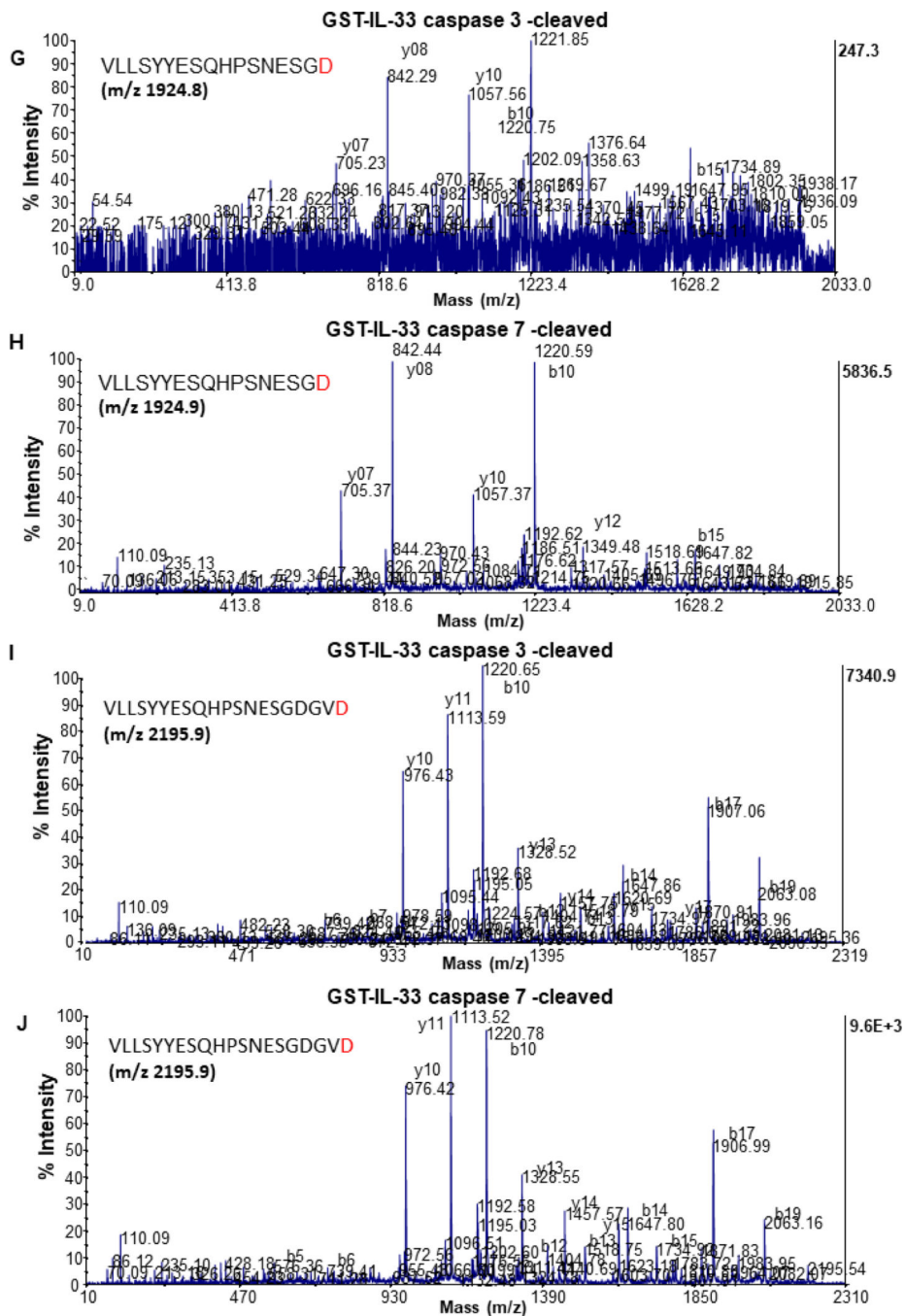
FMK), caspase 3 and 7 inhibitor (Z-DEVD-FMK), or caspase 1 inhibitor (Ac-YVAD-CHO); 50 μ M inactive necrostatin 1 (Inact Ctr); and/or 20 μ M or 50 μ M of necrostatin 1 (NEC-1), necrostatin 5 (NEC-5), necrostatin 7 (NEC-7), or necrostatin 1s (NEC-1s) as indicated. E. Immunoblot analysis of EPC2 cells treated for 8 hours with control medium (Mock), 10 nM of Poly (I:C) or 25 μ g/mL of *A. alternata* (A.Alt), house dustmite (HDM), or *A. fumigatus* (A.Fum) allergen extracts in medium alone or pre-mixed with complete protease inhibitor cocktail (Prot Inhib;Roche see Methods). F-G. LDH (F) and IL-33 (G) release analysis in cell supernatants of EPC2 cells expressing endogenous pIL-33 and exposed to various stimuli. Cells were treated as above (A-E) for 2, 4 and 8 hours as indicated. Lysis control are cells treated with Triton 100 lysis buffer for 45 minutes to determine maximum LDH and IL-33 release (CyQUANT LDH cytotoxicity assay - see Methods). Each data point is a mean of a technical duplicate \pm s.d. of in vitro assays. Statistics were performed by two-way ANOVA with Tukey's multiple comparisons test: p value 0.0003 (***) . H-I. Immunoblot analysis of intracellular IL-33 and cellular components from total cell lysates of cells expressing endogenous pIL-33. H. Immunoblot analysis of control (TLR3 +) and CRISPR/Cas9 TLR3 knockout (TLR3 -) EPC2 cells treated as above (A-E). I. Immunoblot analysis of total cell lysates of human esophageal epithelial cells (EPC2), skin epithelial cells (HaCaT), bronchial epithelial cells (HBEC3-KT) expressing endogenous IL-33, and fibroblasts (FEF3) cells; IL-33 expression in FEF3 cells was induced with 100 pg/mL TNF- α for 16 hours. Then all the cells were incubated with either control medium or 10 nM Poly (I:C)



Extended Data Fig. 2. Peptide profiles of intact and cleaved precursor IL-33

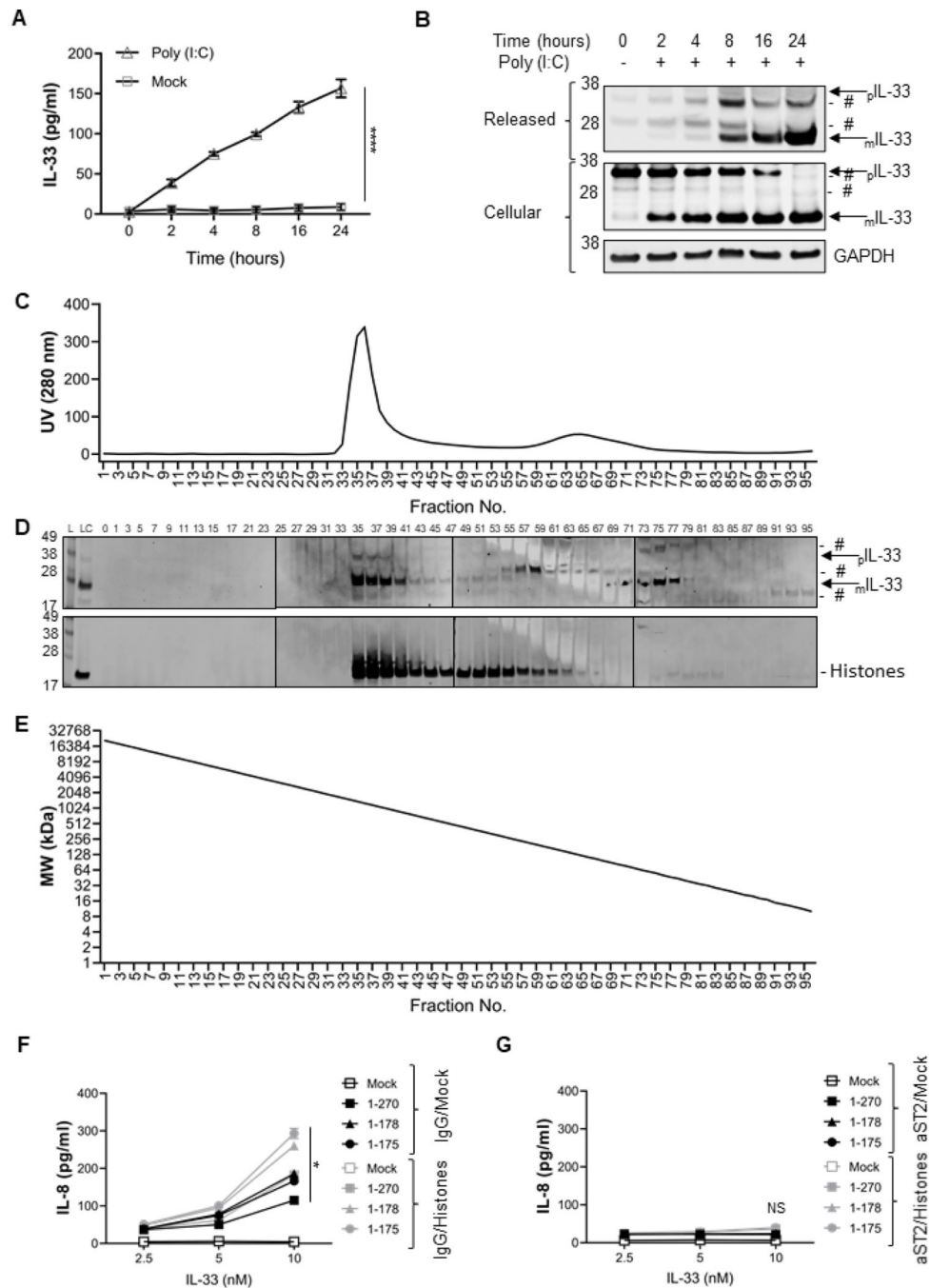
A. Precursor IL-33 reference sequence (UniProtKB O95760). Peptides covered by analysis are underlined. Bold letter Ds indicate residues 175 (left) and 178 (right). B-F. Summary table and peptide profiles of recombinant human IL-33 peptides identified by MALDI-TOF Mass Spectrometry and Tandem Liquid Chromatography MALDI-TOF Mass Spectrometry (LCMS) before and after cleavage by recombinant human caspases. C-F. Exact profiles corresponding to identified peptides sequences of precursor (full-length control; C, E) and cleaved (D, F) GST-IL-33 are labeled with colors in the inserts, and the first letter

of each color in the histogram peptide profiles as indicated: green (G), blue (B), and purple (P). Bold red indicates extra sequence identified by nano-LCMS. G-H. The 159-VLLSYYESQHPSNESGD-175 peptide profiles were generated by caspase 3 and caspase 7 cleavage. I-J. 159-VLLSYYESQHPSNESGDGVD-178 peptide profiles generated by caspase 3 and caspase 7 cleavage, respectively. A-J. Data are a summary of n = 4 independent experiments. m/z, mass-to-charge ratio



Extended Data Fig. 3. Flow cytometry gating strategy for Figure 3 E–G

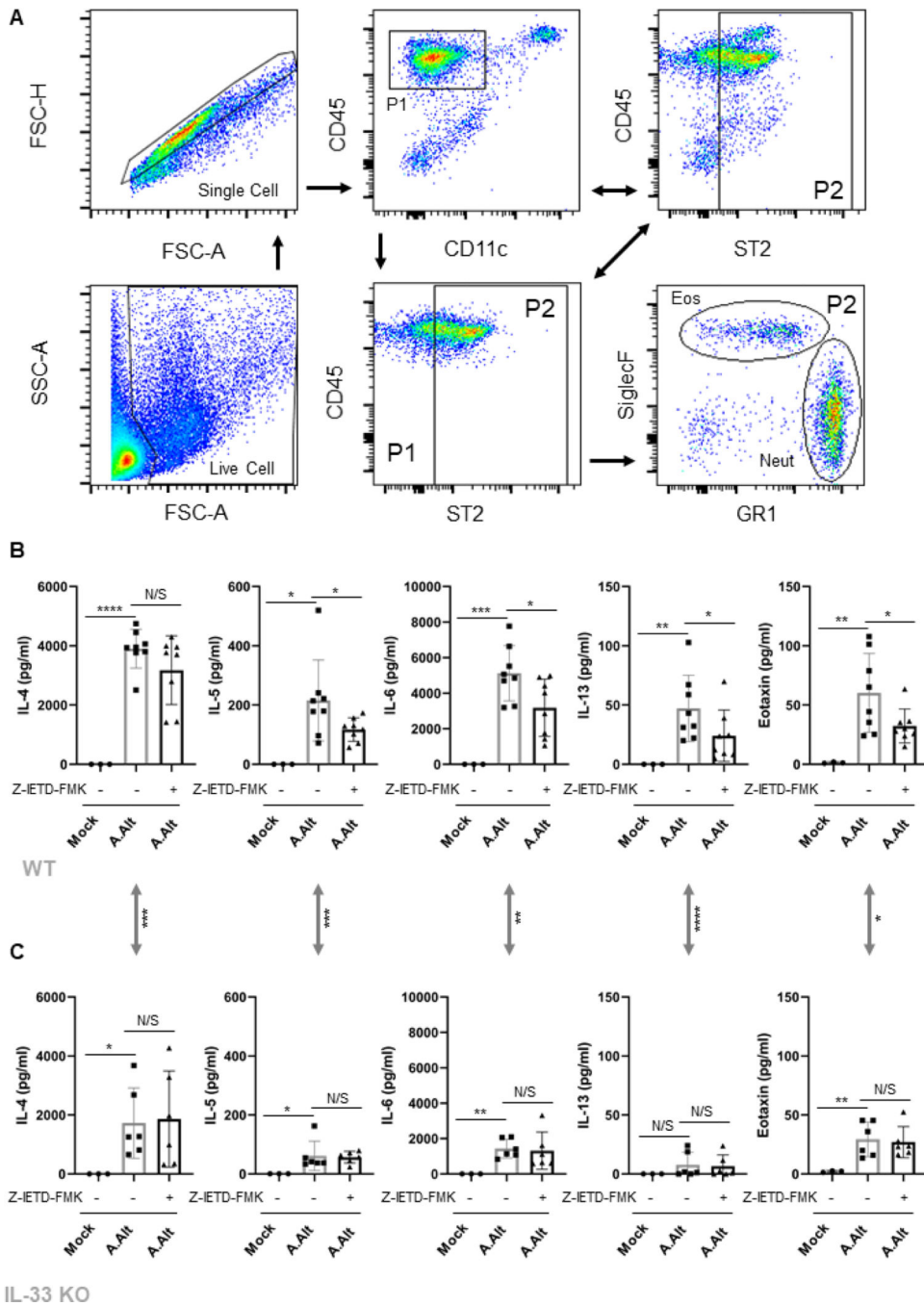
A-D. IL-33 knock out (KO) mice were intraperitoneally injected with equimolar quantities (10 nM) of recombinant pIL-33 and mIL-33 forms in PBS or PBS alone (Mock). Single-cell dot plot data and gating strategy for live, mouse, intraperitoneal cells (A) where P0 are neutrophils (Neut; GR1/Ly6ChighCD11b+c-KIT-) and inflammatory macrophages (iM ϕ ; GR1/Ly6CmediumCD11b+c-KIT-). A-B. Flow cytometry analysis of single-cell dot plot data with corresponding gates (B) for neutrophils (P1; GR1high CD11b+) and inflammatory macrophages (P2; GR1medium CD11b+). Summary plots show neutrophil (C) and inflammatory macrophages (D) influx in peritoneal cavity. Data are representative of n = 3 independent experiments. C-D. Data are summary of n = 3 independent experiments. Each data point is a mean of a technical duplicate \pm SD of in vivo (individual mouse) assays. Statistics were performed by one-way ANOVA with Tukey's multiple comparisons test: p value 0.0001 (****), p value 0.0002 (***), and p value 0.008 (**).



Extended Data Fig. 4. Chromatin-binding domain containing mIL-33 forms are released in complex with histones, which potentiate mIL-33 biological activity

A. Quantification analysis of released (cell medium) IL-33 from TE-7 cells overexpressing pIL-33 (1-270). Cells were treated with control medium or Poly (I:C) (10 nM) for 0–24 hours, and medium was collected for each time point. B. Immunoblot analysis of released (concentrated cell medium) and intracellular (cellular; total cell lysates) IL-33 from the corresponding TE-7 cells. GAPDH was used as a loading control. C. UV absorption plot of size-exclusion column fractions 1–95. D. Immunoblot analysis of TE-7 cells overexpressing pIL-33 (1-270). Cells were treated with TLR3 agonist (Poly (I:C)) for 8 hours in serum-free

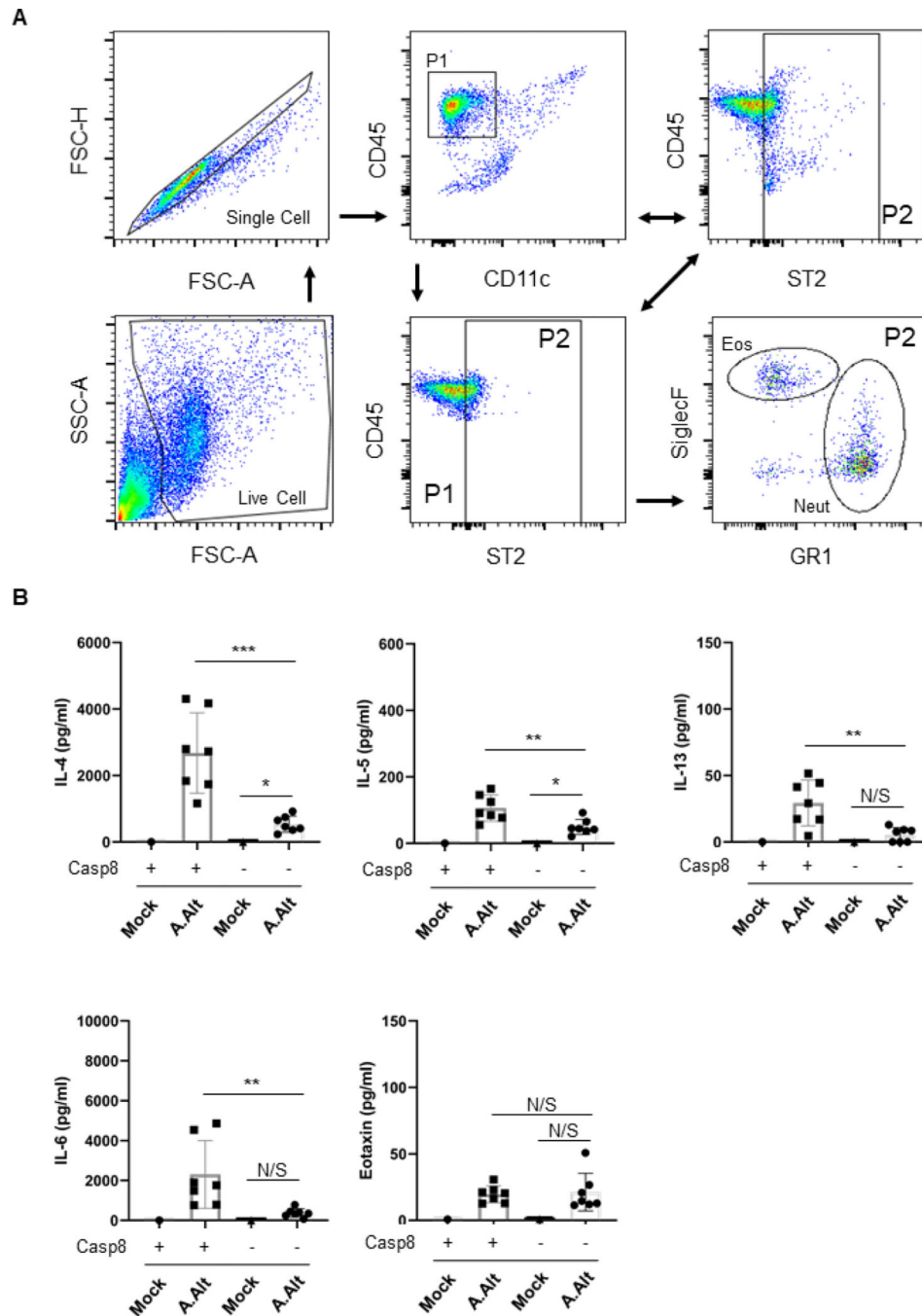
medium (Opti-MEM). Medium containing secreted IL-33 was supplemented with complete protease inhibitors, filtered through 45 μ M pores, DNase treated, and concentrated 10-fold using a 10-kDa cutoff membrane filter. Samples were run on the size-exclusion column. Fractions 1–95 were collected, concentrated 20-fold using a 10-kDa cutoff membrane filter, and analyzed via immunoblotting in the following order: protein standard ladder (L), secreted IL-33 medium loading control (LC), and fractions 1–95. E. Size-exclusion column standard curve by fraction number as a function of molecular weight (MW). F, G. IL-33 bioactivity assay as function of IL-8 secretion by HMC-I human mast cells. Cells were treated for 8 h with 2.5–10 nM of wheat germ extract–produced IL-33 forms in medium alone (Mock) or medium supplemented with 500 ng of acetone-purified histones in the presence of IgG control (IgG) or anti-ST2 blocking antibody (aST2). A–G. Data are representative of $n = 3$ independent experiments. Immunoblot left margin (throughout): protein molecular weight (kDa). Right margin (throughout): protein names (m, mature; p, precursor); # are non-specific bands. A, F, G. Each data point is a mean of a technical duplicate \pm SD. Statistics were performed by 2-way ANOVA with Tukey’s multiple comparisons test: p value 0.0001 (****) and p value 0.015 (*).



Extended Data Fig. 5. Flow cytometry gating strategy and BALF cytokines for Figure 4 D-I

A. Single-cell dot plot data and gating strategy for the live, mouse bronchoalveolar fluid (BALF) cells: the P1 CD45⁺CD11c⁻ population is derived from total single cells; the P2 population was identified on the basis of total single cells and applied on the P1 population. Finally, the P2-derived ST2⁺ cells are neutrophils (Neut; SiglecF⁺GR1^{high}/Ly6Chigh) and eosinophils (Eos; SiglecF⁺GR1^{low}/Ly6Cmedium/low). Data are representative of n = 3 independent experiments. B-C. BALF cytokines in WT (B) and IL-33 KO (C) mice were measured by ELISA with and without treatment with a specific inhibitor of caspase

8 (Z-IETD-FMK). Data are summary of n = 3 independent experiments. Each data point is a mean ± SD of in vivo (individual mouse) assays. Statistics were performed by unpaired t-test: p value 0.0001 (****), p value 0.0067 (***), p value 0.0099 (**), p value 0.0431 (*). N/S is not significant. Arrowheads are comparison of *A. alternata* challenges alone between WT and IL-33 KO mice. Statistics were performed by unpaired one-sided t-test: p value 0.0001 (****), p value 0.0006 (***), p value 0.0034 (**), p value 0.028 (*).



Extended Data Fig. 6. Flow cytometry gating strategy and BALF cytokines for Figure 5 D–E

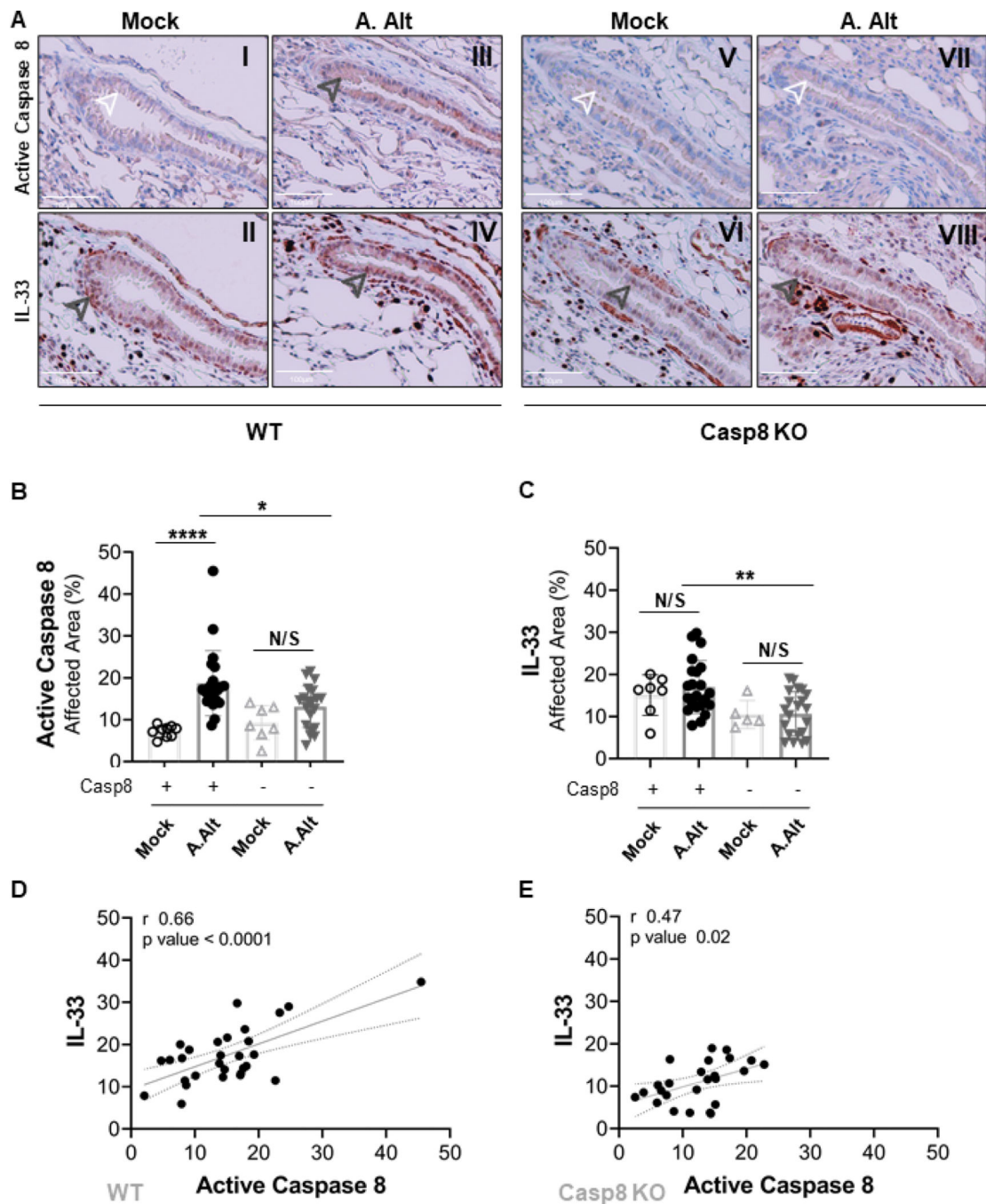
A. Single-cell dot plot data and gating strategy for live BALF cells (D, E): the P1 CD45+CD11c- population is derived from total single cells; the P2 population was identified on the basis of total single cells and applied on the P1 population. Finally, the P2-derived ST2+ cells are neutrophils (Neut; SiglecF-GR1/Ly6Chigh) and eosinophils (Eos; SiglecF+GR1/Ly6Cmedium/low). Data are representative of n = 3 independent experiments. B. BALF cytokines in WT and caspase 8 KO mice were measured by ELISA. Data are summary of n = 3 independent experiments. Each data point is a mean ± SD of in vivo (individual mouse) assays. Statistics were performed by unpaired one-sided t-test: p value 0.0003 (***), p value 0.0058 (**), p value 0.0442 (*). N/S is not significant.

Author Manuscript

Author Manuscript

Author Manuscript

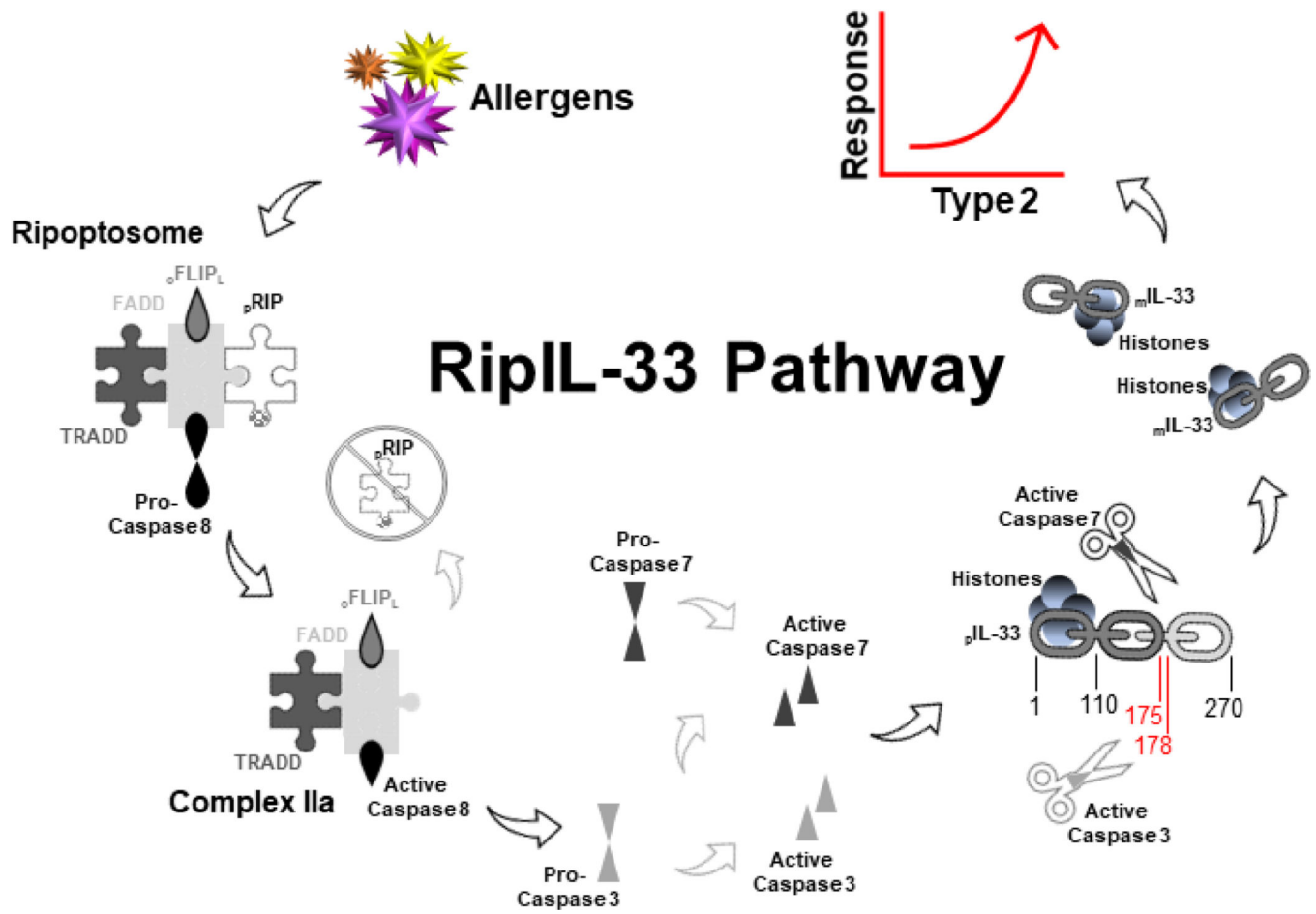
Author Manuscript



Extended Data Fig. 7. Active caspase 8 and IL-33 interaction in airway inflammation

A-E. Wildtype (WT; +) and caspase 8 knock out (KO; -) mice were treated intratracheally with *A. alternata* (A.Alt) extract in PBS or PBS alone (Mock) - see Figure 5. A. Representative images of active caspase 8 and IL-33 staining in murine lungs bronchi epithelial cells in mice treated with PBS (Mock) and *A. alternata* (A.Alt). Positive (grey) and negative (white) staining is indicated with arrowheads. The 100 μ m scale bars included in all images. B. Active caspase 8 quantification. C. IL-33 quantification. D-E. Correlation of IL-33 with active caspase 8 in WT (D) and caspase 8 KO (E) mice. Statistics are by

Pearson correlation (D-E): R2 (r) and p values are as indicated. Data are representative (A) or a summary (B-E) of n = 3 independent experiments. Each data point is a mean \pm SD of multiple sections measurement in an individual mouse. Statistics were performed by one-way ANOVA with Tukey's multiple comparisons test: p-value 0.0001 (****), p value 0.0025 (**), p value 0.0139 (*). N/S is not significant.



Extended Data Fig. 8. RipIL-33 pathway for environmental allergen sensing

Allergen exposure triggers RIP phosphorylation and ripoosome assembly: RIP (RIP) in complex with cFLIP_L, FADD, TRADD, and pro-caspase 8. Following RIP phosphorylation (pRIP), FADD-bound pro-caspase 8 is self-cleaved and activated. Active caspase 8 cleaves and deactivates pRIP and activates effector pro-caspases 3 and 7. Active effector caspases in turn target and cleave histone-bound pIL-33 at amino acids D175 and D178. mIL-33 is released to initiate type 2 innate immune responses.

Supplementary Material

Refer to Web version on PubMed Central for supplementary material.

Acknowledgements

This work was supported in part by NIH R37 AI045898; the Campaign Urging Research for Eosinophilic Disease (CURED); and the Sunshine Charitable Foundation and its supporters, Denise and David Bunning (M.E.R.). By R01 AI123176, R01 AI113125 and R01 CA231303 (C.P.). The authors thank Shawna Hottinger for editorial assistance.

References

1. Galli SJ, Nakae S. & Tsai M. Mast cells in the development of adaptive immune responses. *Nat Immunol* 6, 135–142 (2005). [PubMed: 15662442]
2. Trompette A. et al. Allergenicity resulting from functional mimicry of a Toll-like receptor complex protein. *Nature* 457, 585–588 (2009). [PubMed: 19060881]
3. Gowthaman U. et al. Identification of a T follicular helper cell subset that drives anaphylactic IgE. *Science* 365 (2019).
4. Jain A. et al. T cells instruct myeloid cells to produce inflammasome-independent IL-1beta and cause autoimmunity. *Nat Immunol* 21, 65–74 (2020). [PubMed: 31848486]
5. Hill AA & Diehl GE Identifying the Patterns of Pattern Recognition Receptors. *Immunity* 49, 389–391 (2018). [PubMed: 30231979]
6. Pasare C. & Medzhitov R. Toll-dependent control mechanisms of CD4 T cell activation. *Immunity* 21, 733–741 (2004). [PubMed: 15539158]
7. Gour N. et al. Dysregulated invertebrate tropomyosin-dectin-1 interaction confers susceptibility to allergic diseases. *Sci Immunol* 3 (2018).
8. Wills-Karp M. et al. Trefoil factor 2 rapidly induces interleukin 33 to promote type 2 immunity during allergic asthma and hookworm infection. *J Exp Med* 209, 607–622 (2012). [PubMed: 22329990]
9. Cayrol C. et al. Environmental allergens induce allergic inflammation through proteolytic maturation of IL-33. *Nat Immunol* 19, 375–385 (2018). [PubMed: 29556000]
10. Dolence JJ et al. Airway exposure initiates peanut allergy by involving the IL-1 pathway and T follicular helper cells in mice. *J Allergy Clin Immunol* 142, 1144–1158 e1148 (2018).
11. Lambrecht BN & Hammad H. The airway epithelium in asthma. *Nat Med* 18, 684–692 (2012). [PubMed: 22561832]
12. Martin NT & Martin MU Interleukin 33 is a guardian of barriers and a local alarmin. *Nat Immunol* 17, 122–131 (2016). [PubMed: 26784265]
13. Cayrol C. & Girard JP Interleukin-33 (IL-33): A nuclear cytokine from the IL-1 family. *Immunol Rev* 281, 154–168 (2018). [PubMed: 29247993]
14. Cherry WB, Yoon J, Bartemes KR, Iijima K. & Kita H. A novel IL-1 family cytokine, IL-33, potently activates human eosinophils. *J Allergy Clin Immunol* 121, 1484–1490 (2008). [PubMed: 18539196]
15. Grotenboer NS, Ketelaar ME, Koppelman GH & Nawijn MC Decoding asthma: translating genetic variation in IL33 and IL1RL1 into disease pathophysiology. *J Allergy Clin Immunol* 131, 856–865 (2013). [PubMed: 23380221]
16. Schmitz J. et al. IL-33, an interleukin-1-like cytokine that signals via the IL-1 receptor-related protein ST2 and induces T helper type 2-associated cytokines. *Immunity* 23, 479–490 (2005). [PubMed: 16286016]
17. Nelson AM et al. dsRNA Released by Tissue Damage Activates TLR3 to Drive Skin Regeneration. *Cell Stem Cell* 17, 139–151 (2015). [PubMed: 26253200]
18. Codina R, Roby MD & Esch RE Endotoxin Testing of Allergen Extracts. *J Allergy Clin Immunol* 123, S97–S97 (2009).
19. Bressenot A. et al. Assessment of apoptosis by immunohistochemistry to active caspase-3, active caspase-7, or cleaved PARP in monolayer cells and spheroid and subcutaneous xenografts of human carcinoma. *J Histochem Cytochem* 57, 289–300 (2009). [PubMed: 19029405]

20. Kaczmarek A, Vandenaabee P. & Krysko DV Necroptosis: the release of damage-associated molecular patterns and its physiological relevance. *Immunity* 38, 209–223 (2013). [PubMed: 23438821]
21. Tummers B. & Green DR Caspase-8: regulating life and death. *Immunol Rev* 277, 76–89 (2017). [PubMed: 28462525]
22. Lingel A. et al. Structure of IL-33 and its interaction with the ST2 and IL-1RAcP receptors--insight into heterotrimeric IL-1 signaling complexes. *Structure* 17, 1398–1410 (2009). [PubMed: 19836339]
23. Liu X. et al. Structural insights into the interaction of IL-33 with its receptors. *P Natl Acad Sci USA* 110, 14918–14923 (2013).
24. Travers J. et al. Chromatin regulates IL-33 release and extracellular cytokine activity. *Nat Commun* 9, 3244 (2018). [PubMed: 30108214]
25. Bouffi C. et al. IL-33 markedly activates murine eosinophils by an NF-kappaB-dependent mechanism differentially dependent upon an IL-4-driven autoinflammatory loop. *J Immunol* 191, 4317–4325 (2013). [PubMed: 24043894]
26. Enoksson M. et al. Intraperitoneal influx of neutrophils in response to IL-33 is mast cell-dependent. *Blood* 121, 530–536 (2013). [PubMed: 23093619]
27. Dellon ES et al. Updated International Consensus Diagnostic Criteria for Eosinophilic Esophagitis: Proceedings of the AGREE Conference. *Gastroenterology* 155, 1022–1033 e1010 (2018).
28. Kallenberger SM et al. Intra- and interdimeric caspase-8 self-cleavage controls strength and timing of CD95-induced apoptosis. *Sci Signal* 7, ra23 (2014).
29. Dinarello CA Overview of the IL-1 family in innate inflammation and acquired immunity. *Immunol Rev* 281, 8–27 (2018). [PubMed: 29247995]
30. Snelgrove RJ et al. *Alternaria*-derived serine protease activity drives IL-33-mediated asthma exacerbations. *J Allergy Clin Immunol* 134, 583–592 e586 (2014).
31. Hammad H. et al. House dust mite allergen induces asthma via Toll-like receptor 4 triggering of airway structural cells. *Nat Med* 15, 410–416 (2009). [PubMed: 19330007]
32. Novak N. & Bieber T. Allergic and nonallergic forms of atopic diseases. *J Allergy Clin Immunol* 112, 252–262 (2003). [PubMed: 12897728]
33. Komai-Koma M. et al. Interleukin-33 amplifies IgE synthesis and triggers mast cell degranulation via interleukin-4 in naive mice. *Allergy* 67, 1118–1126 (2012). [PubMed: 22702477]
34. Bossaller L. et al. Cutting edge: FAS (CD95) mediates noncanonical IL-1beta and IL-18 maturation via caspase-8 in an RIP3-independent manner. *J Immunol* 189, 5508–5512 (2012). [PubMed: 23144495]
35. Dusek RL et al. The differentiation-dependent desmosomal cadherin desmoglein 1 is a novel caspase-3 target that regulates apoptosis in keratinocytes. *J Biol Chem* 281, 3614–3624 (2006). [PubMed: 16286477]
36. Straumann A. et al. Budesonide Is Effective in Adolescent and Adult Patients With Active Eosinophilic Esophagitis. *Gastroenterology* 139, 1526–+ (2010).
37. Gunther S. et al. IL-1 Family Cytokines Use Distinct Molecular Mechanisms to Signal through Their Shared Co-receptor. *Immunity* 47, 510–523 e514 (2017).
38. Luzina IG et al. Full-length IL-33 promotes inflammation but not Th2 response in vivo in an ST2-independent fashion. *J Immunol* 189, 403–410 (2012). [PubMed: 22634619]
39. Lefrancais E. et al. Central domain of IL-33 is cleaved by mast cell proteases for potent activation of group-2 innate lymphoid cells. *Proc Natl Acad Sci U S A* 111, 15502–15507 (2014).
40. Bae S. et al. Contradictory functions (activation/termination) of neutrophil proteinase 3 enzyme (PR3) in interleukin-33 biological activity. *J Biol Chem* 287, 8205–8213 (2012). [PubMed: 22270365]
41. Dinarello CA An IL-1 family member requires caspase-1 processing and signals through the ST2 receptor. *Immunity* 23, 461–462 (2005). [PubMed: 16286013]
42. Hudson CA et al. Induction of IL-33 expression and activity in central nervous system glia. *J Leukoc Biol* 84, 631–643 (2008). [PubMed: 18552204]

43. Li H, Willingham SB, Ting JP & Re F. Cutting edge: inflammasome activation by alum and alum's adjuvant effect are mediated by NLRP3. *J Immunol* 181, 17–21 (2008). [PubMed: 18566365]
44. Iwata A. et al. A broad-spectrum caspase inhibitor attenuates allergic airway inflammation in murine asthma model. *J Immunol* 170, 3386–3391 (2003). [PubMed: 12626599]
45. Chinthrajah S. et al. Phase 2a randomized, placebo-controlled study of anti-IL-33 in peanut allergy. *JCI Insight* 4 (2019).
46. Cayrol C. & Girard JP IL-33: an alarmin cytokine with crucial roles in innate immunity, inflammation and allergy. *Curr Opin Immunol* 31, 31–37 (2014). [PubMed: 25278425]
47. Byers DE et al. Long-term IL-33-producing epithelial progenitor cells in chronic obstructive lung disease. *J Clin Invest* 123, 3967–3982 (2013). [PubMed: 23945235]
48. Hardman CS, Panova V. & McKenzie AN IL-33 citrine reporter mice reveal the temporal and spatial expression of IL-33 during allergic lung inflammation. *Eur J Immunol* 43, 488–498 (2013). [PubMed: 23169007]
49. Sherrill JDet al. Desmoglein-1 regulates esophageal epithelial barrier function and immune responses in eosinophilic esophagitis. *Mucosal Immunol* 7, 718–729 (2014). [PubMed: 24220297]
50. Luthi AU et al. Suppression of interleukin-33 bioactivity through proteolysis by apoptotic caspases. *Immunity* 31, 84–98 (2009). [PubMed: 19559631]

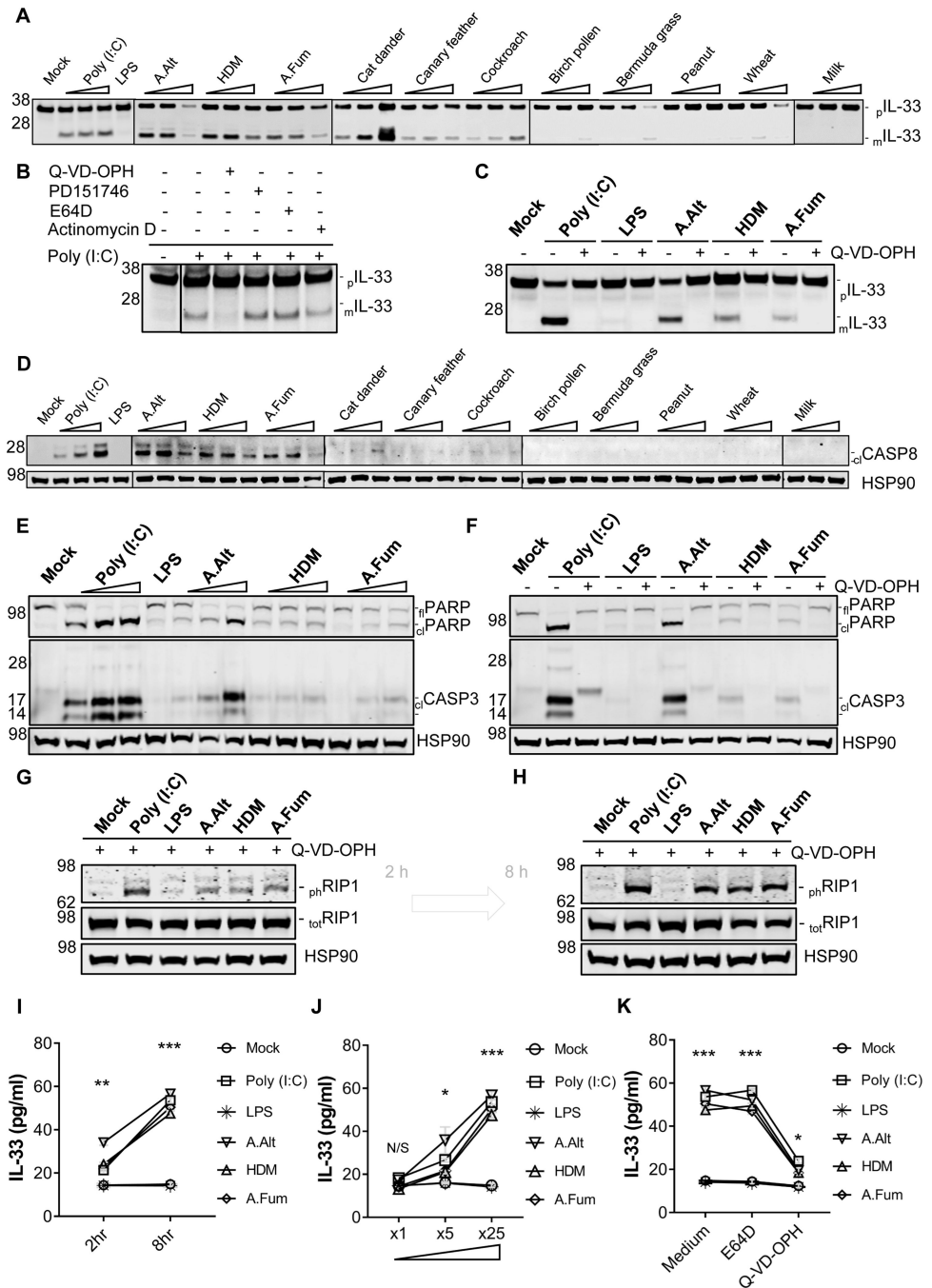


Figure 1. Effect of environmental allergens on riptosome-dependent, intracellular pIL-33 maturation and release

A-H. Immunoblot analysis of intracellular IL-33 and cellular components from total cell lysates of cells expressing endogenous pIL-33 and exposed to various environmental allergens. Left margin (throughout): protein molecular weight (kDa). Right margin (throughout): protein names (cl, cleaved; fl, full length; m, mature; p, precursor; tot, total; ph, phosphorylated). EPC2 cells were incubated with control medium alone (Mock), 0.4 nM (A, D, E), 2 nM (A, D, E) or 10 nM (A-K) of Poly (I:C); or 10 nM Poly(I:C) or LPS (A-K);

1 µg/mL (A, D, E), 5 µg/mL (A, D, E), or 25 µg/mL (A-K) of *A. alternata* (A.Alt), house dust mite (HDM), *A. fumigatus* (A.Fum), cat dander, canary feathers, cockroach, birch pollen, Bermuda grass, peanut, whole wheat or cow milk extracts for 8 hours. **B, C, F-H, K.** Cells were treated with control medium or 20 µM pan-caspase inhibitor (Q-VD-OPH), selective calpain inhibitor (PD151746), cysteine protease inhibitor (E64D), or transcription inhibitor (actinomycin D) for 2 (G) or 8 (B, C, F, H, K) hours. **I-K.** Quantification of extracellular IL-33 released from cells overexpressing pIL-33. **A-K.** Data are representative or a summary of n = 3 independent experiments. Each data point is a mean of a technical duplicate ± SD from in vitro assays. Statistics were performed by 2-way ANOVA with Tukey's multiple comparisons test: p value 0.0007 (***), p value 0.003 (**), and p value 0.03 (*), N/S, not significant.

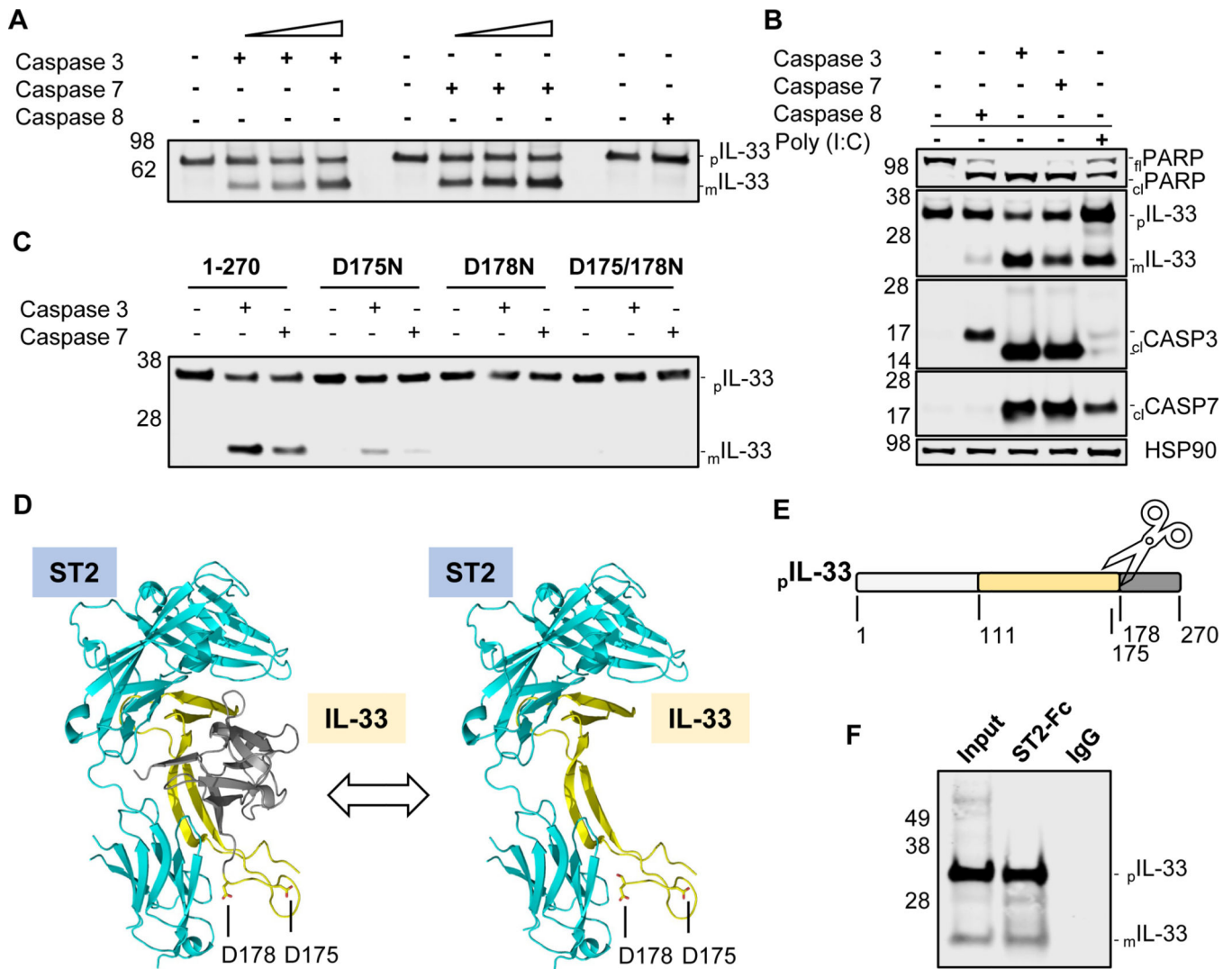


Figure 2. Effect of caspase 3 and 7 on proteolytic maturation of pIL-33 and ST2-interacting mIL-33 forms

A. Immunoblot analysis of recombinant IL-33 (100 ng) incubated for 2 hours with control medium or 10, 30, or 100 units of recombinant human active caspases 3, 7 or 8 (100 units). **B.** Immunoblot analysis of necrotic supernatants of TE-7 cells overexpressing pIL-33 (1–270). Cells were pre-incubated with control medium or Poly (I:C) (10 nM) for 8 hours. Control supernatants were incubated with medium or 100 units of recombinant human active caspases 3, 7, or 8 for 2 hours. **C.** Immunoblot analysis of TE-7 cells overexpressing wildtype (1–270), single-point mutated (D175N; D178N), and double-point mutated (D175N/D178N) pIL-33. Necrotic supernatants were incubated with control medium or 100 units of recombinant human active caspases 3 or 7 for 2 hours. **D.** X-ray complex structure of ST2 receptor (S117-S268; PDB ID: 4KC3) juxtaposed with the NMR-based structure of IL-33 (S111-T270; PDB ID: 2KLL) showing IL-33 minimal binding domain interacting with ST2 and the non-interacting IL-33 flexible loop with a.a. D175 and D178 (yellow); D179-T270 is posterior to the IL-33 and is not interacting with ST2 receptor binding interface (grey). **E.** Schematic representation of (D) inclusive of the M1-H109 and

caspace cleavage site (D175, D178) as determined by MS/tandem LC-MS. **F.** Immunoblot analysis of coimmunoprecipitation of IL-33 and ST2: TE-7 cells overexpressing pIL-33 (1–270) were incubated with Poly (I:C) (10 nM) for 8 hours and lysed. Lysate input control (left) and co-immunoprecipitation of IL-33 with ST2-Fc (middle) or normal goat IgG (right) are shown. **A-C, F.** Data are representative of n = 3 independent experiments. Left margin (throughout): protein molecular weight (kDa). Right margin (throughout): protein names (cl, cleaved; fl, full length; m, mature; p, precursor).

Author Manuscript

Author Manuscript

Author Manuscript

Author Manuscript

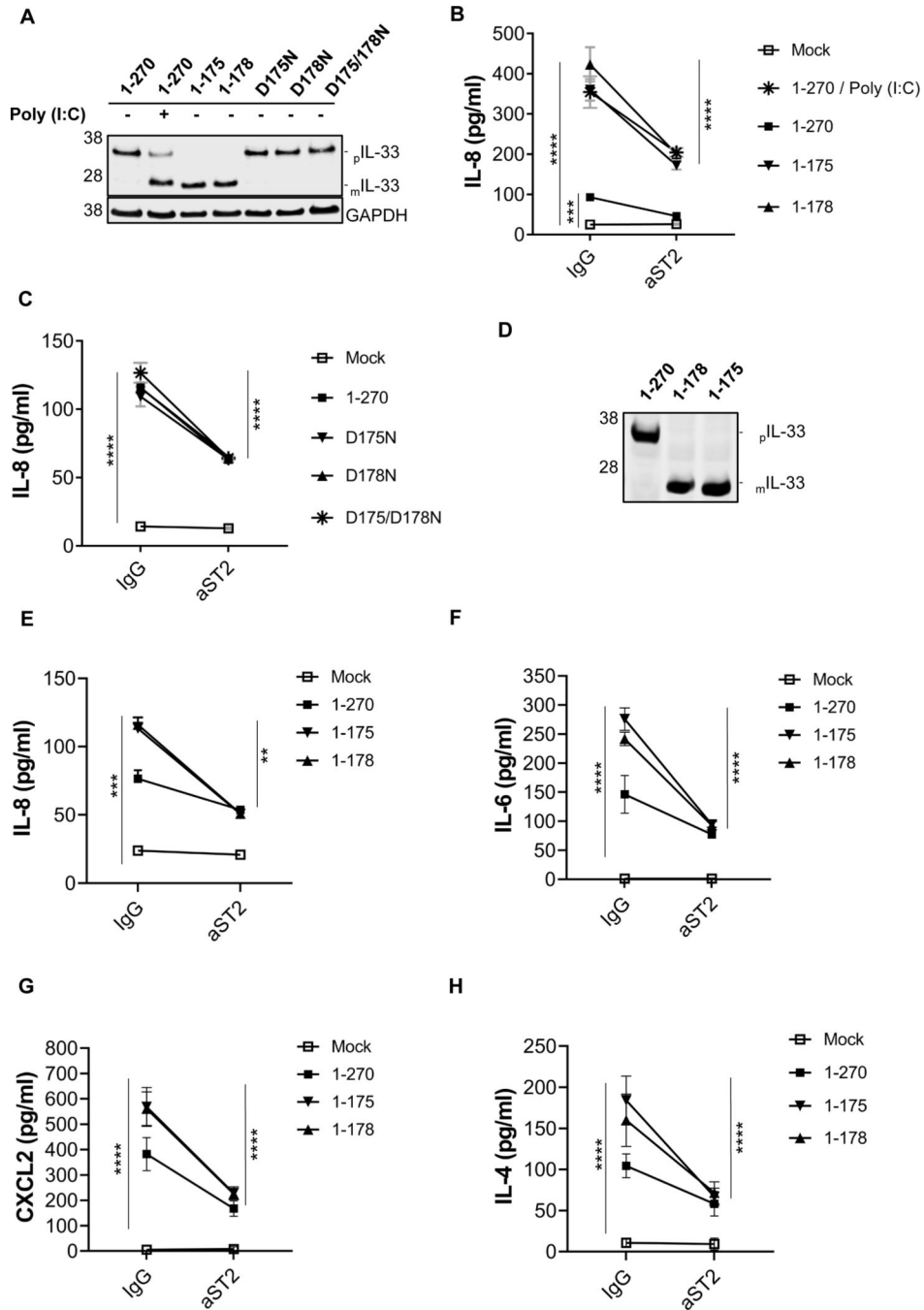


Figure 3. IL-33 bioactivity as a function of G176–270T c-terminal domain

A. Immunoblot analysis of TE-7 cells overexpressing WT pIL-33 (1–270) and mIL-33 forms (1–175; 1–178) or single-point mutated (D175N; D178N) or double-point mutated (D175N/D178N) pIL-33 (1–270). Cells were treated with control medium or TLR3 agonist (Poly (I:C); 10 nM) for 8 hours and lysed. **B–C.** IL-33 bioactivity assay as a function of IL-8 secretion by HMC-I human mast cells with and without ST2 neutralization (anti-ST2 antibody and control IgG). TE-7 cells overexpressing IL-33 (same as A) were incubated with control medium or Poly (I:C) (10 nM) for 8 hours. Then HMC-I cells

were co-incubated with medium alone (Mock), normalized necrotic supernatants from the TE-7 cells (A): 1–270 expressing cells treated with Poly(I:C) (1–270/Poly(I:C); containing both _pIL-33 and secreted _mIL-33 forms), untreated 1–270, 1–175, 1–178, D175N, D178N and D175/D178N expressing cells for 8 hours. The IL-8 concentration in the medium was measured by ELISA. **D.** Immunoblot analysis of recombinant IL-33 as used in (E) **E.** IL-33 bioactivity assay as a function of IL-8 secretion by HMC-I human mast cells with ST2 neutralization (anti-ST2 antibody) and control IgG. Cells were treated for 8 hours with equimolar quantities (10 nM) of recombinant IL-33 forms (same as D) in medium or medium alone (Mock). **F-H.** Primary murine eosinophils were stimulated with ST2 neutralization (anti-ST2 antibody) and control IgG. Cells were treated for 18 hours with equimolar quantities (10 nM) of recombinant IL-33 forms (same as D) in medium or medium alone (Mock). The cytokines concentrations were measured by ELISA. **A-E.** Data are representative of n = 3 independent experiments. **A-D.** Left margin (throughout): protein molecular weight (kDa). Right margin (throughout): protein names (m, mature; p, precursor). **F-H.** Data are summary of n = 3 independent experiments. **B, C, E-H.** Each data point is a mean of a technical duplicate ± SD from the in vitro assays. Statistics were performed by 2-way ANOVA with Tukey's multiple comparisons test: p value 0.0001 (****), p value 0.0007 (***), and p value 0.0013 (**).

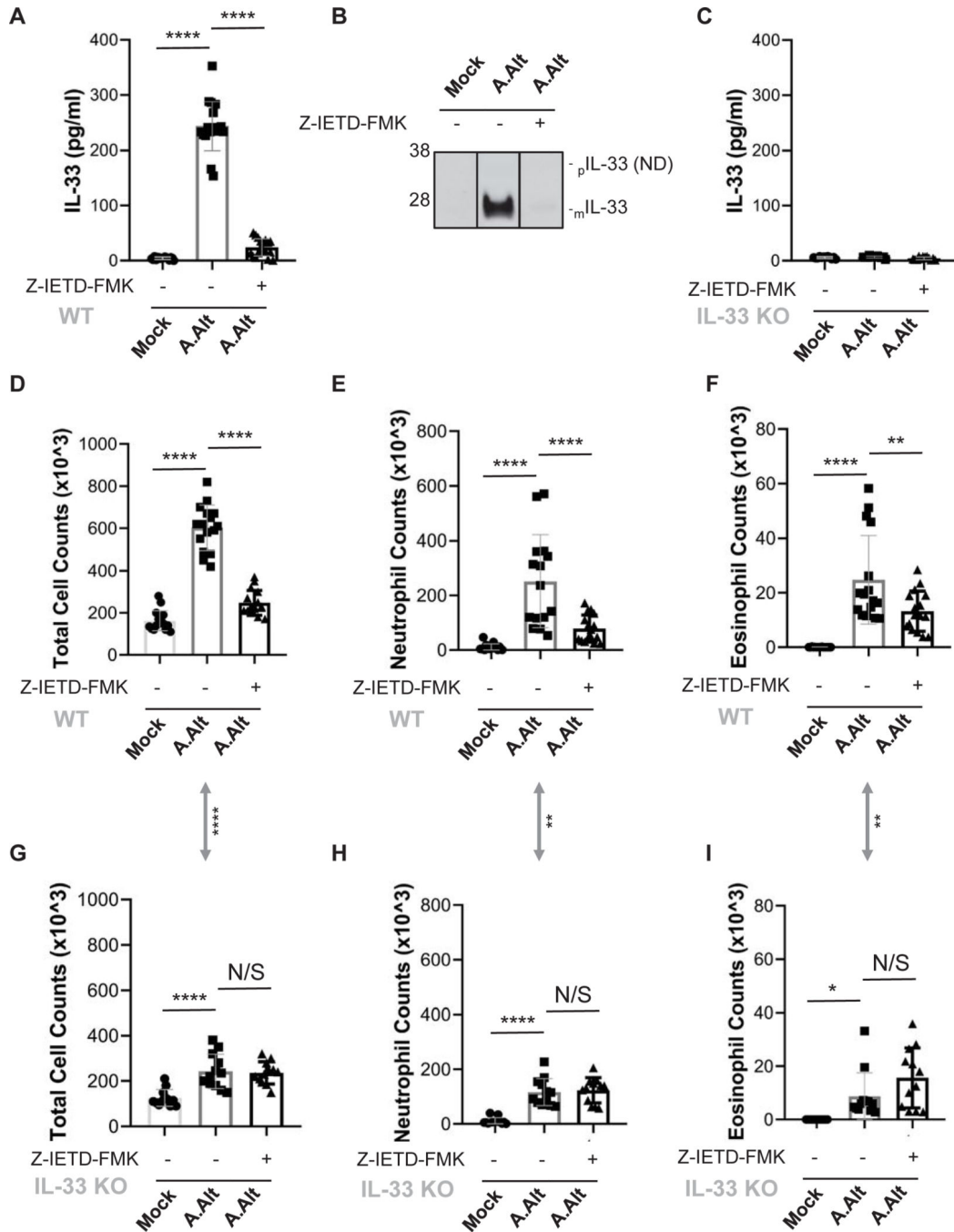


Figure 4. Effect of ripoptosome inhibition on IL-33-dependent airway inflammation

A-I. Wildtype (WT; A, B, D-F) and IL-33 knock out (KO; A-C, G-I) mice were treated intratracheally with *A. alternata* (A.Alt) extract in PBS or PBS alone (Mock). Mice were challenged three consecutive times 24 hours apart and sacrificed 4 hours after the last challenge. Mice were IV injected with vehicle (PBS, DMSO 0.1%) alone (Mock) or with a caspase 8-specific inhibitor preparation (Z-IETD-FMK; PBS, DMSO 0.1%) 1 hour before and after each *A. alternata* challenge. **A-C.** ELISA quantification (A, C) and immunoblot (B) analysis of secreted _mIL-33 in bronchoalveolar lavage fluid (BALF) from WT (A,

B) and IL-33 KO (B, C) mice. p IL-33 was not detected (ND). **D-I.** Total BALF cells counts (D, G) and flow cytometry analysis of BALF ST2-positive neutrophils (E, H) and eosinophils (F, I). From WT (D-F) and IL-33 KO (G-I) mice. Data are representative (B) or a summary (A, C-I) of $n = 3$ independent experiments. Immunoblot (B) left margin (throughout): protein molecular weight (kDa). Right margin (throughout): protein names (m, mature; p, precursor). Each data point is a mean of a technical duplicate \pm SD of in vivo (individual mouse) assays. Statistics were performed by one-way ANOVA with Tukey's multiple comparisons test: p value 0.0001 (****), p value 0.008 (**), and p value 0.03 (*), N/S, not significant. Arrowheads are comparison of *A. alternata* challenges alone between WT and IL-33 KO mice. Statistics were performed by unpaired one-sided t-test: p value 0.0001 (****), p value 0.0067 (**).

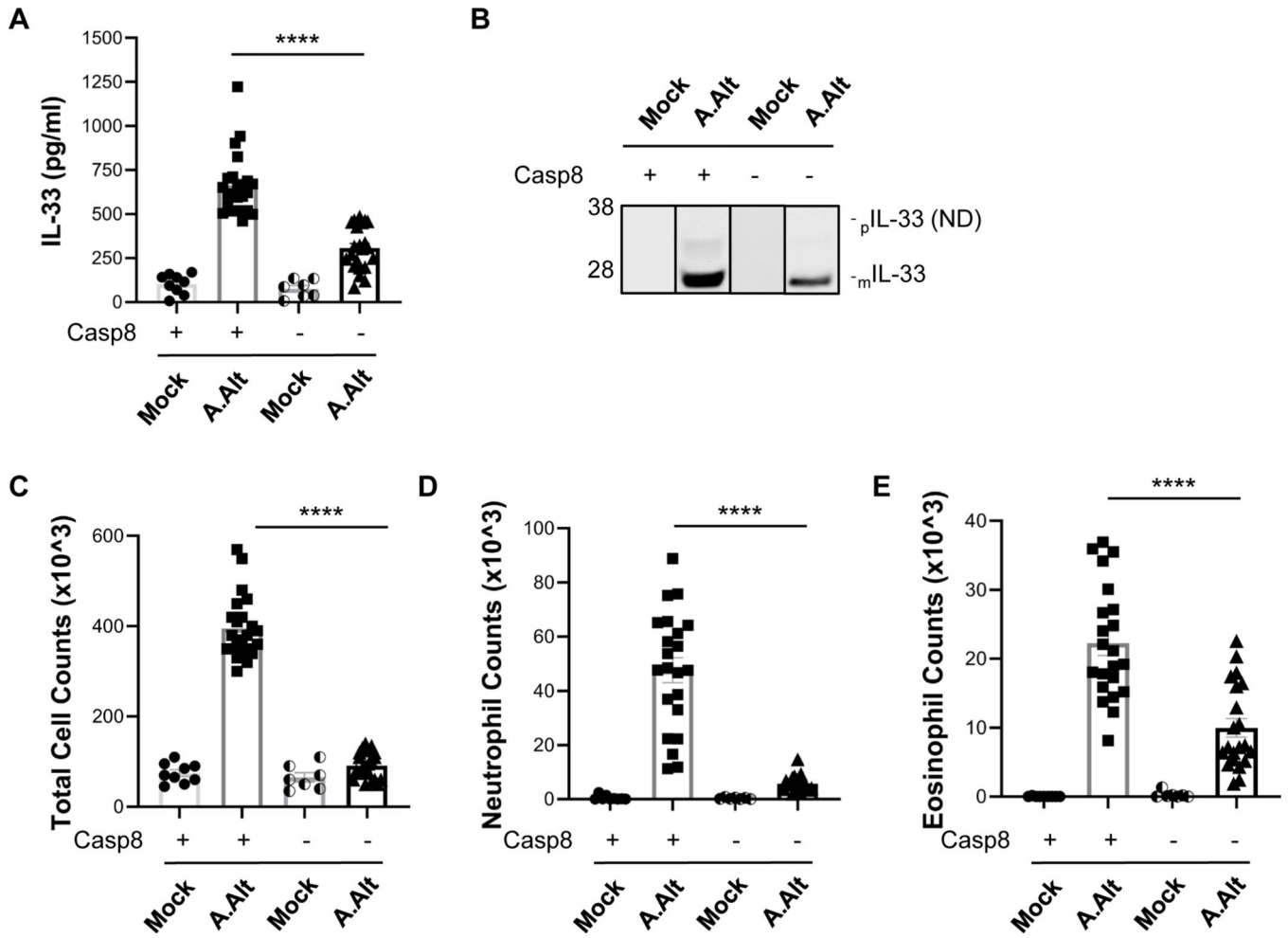


Figure 5. Effect of caspase 8 on allergic airway inflammation

A-F. Wildtype (WT; +) and caspase 8 knock out (KO; -) mice were treated intratracheally with *A. alternata* (A.Alt) extract in PBS or PBS alone (Mock). Caspase 8 KO mice had targeted deletion of caspase 8 in bronchial epithelial cells by generating CC10-CreER^{+/-}/Casp8^{fl/fl} mice (see Methods). Mice were challenged three consecutive times 24 hours apart and sacrificed 4 hours after the last challenge. **A-B.** ELISA quantification (A) and immunoblot (B) analysis of secreted mIL-33 in bronchoalveolar lavage fluid (BALF). pIL-33 was not detected (ND). **C-E.** Total BALF cells counts (C) and flow cytometry analysis of BALF ST2-positive neutrophils (D) and eosinophils (E). Data are representative (B) or a summary (A, C-E) of n = 3 independent experiments. Immunoblot (B) left margin: protein molecular weight (kDa). Right margin: protein names (m, mature; p, precursor). Each data point is a mean of a technical duplicate ± SD of in-vivo (individual mouse) assays. Statistics were performed by one-way ANOVA with Tukey's multiple comparisons test: p-value 0.0001 (****).

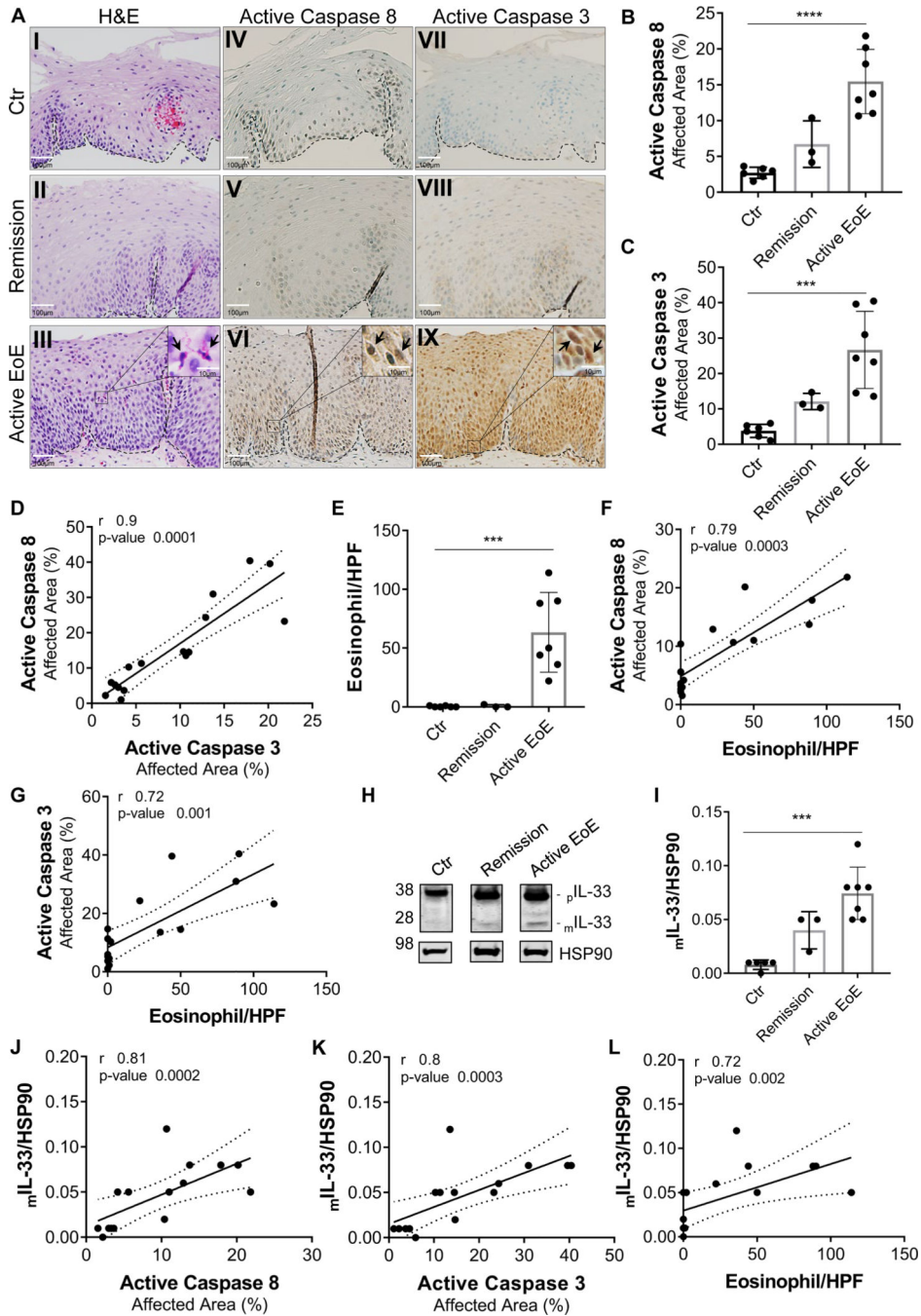


Figure 6. Ripoptosome activation relationship with mIL-33 expression and eosinophilia in EoE
A. Representative images of hematoxylin and eosin (H&E, I-III), active caspase 8 (IV-VI), and active caspase 3 (VII-IX) staining of esophageal biopsies from control individuals (ctr; I, IV, VII) and patients with EoE in remission (II, V, VIII) or active EoE (III, VI, IX). Scale bars, 100 μm in all images and 10 μm in all enlarged regions of interest. The dashed line represents the basement membrane. The enlarged region of interest with scale bars shows eosinophils per high power field (HPF) (III) and active caspase 8 (VI)- or active caspase 3 (IX)-positive cells. **B.** Active caspase 8 quantification. **C.** active caspase 3 quantification. **D.**

Correlation of active caspase 8 with active caspase 3. **E.** Eosinophil quantification per high power field (HPF) from H&E images. **F.** Correlation of active caspase 8 with eosinophil counts. **G.** Correlation of active caspase 3 with eosinophil counts. **H.** Representative immunoblot analysis of esophageal biopsy protein lysates from control individuals and patients with EoE in remission or active EoE. Left margin: protein molecular weight (kDa). Right margin: protein names (m, mature; p, precursor). **I.** $mIL-33$ quantification of immunoblots (H). HSP90 is used as a loading control for $mIL-33$. **J.** Correlation of $mIL-33$ with active caspase 8. **K.** Correlation of $mIL-33$ with active caspase 3. **L.** Correlation of $mIL-33$ with eosinophil counts. **A-L.** Data are from $n = 6$ control individuals, $n = 3$ patients with EoE in remission, and $n = 7$ patients with active EoE. Statistics are by Pearson (E) and Spearman correlation (F, G, J-L): R^2 (r) and p values are as indicated. Each data point is a single data point for an individual biopsy measurement mean \pm SD. Statistics were performed by 2-way ANOVA with Tukey's multiple comparisons test (B, C, E, I): **** $P < 0.0001$ and *** $P < 0.0005$.